Procedures

We did RNA labelling and hybridisation on microRNA microarray chips and undertook postprocessing, as described previously.[13,15,19–21] Briefly, 5 μg of total RNA from every sample was reverse transcribed with biotin end-labelled random-octamer oligonucleotide primers. Hybridisation of biotin-labelled complementary DNA was done on the Ohio State University custom microRNA microarray chip (OSU_CCC version 3.0; ArrayExpress [European Bioinformatics Institute, Cambridge, UK], array design A-MEXP-620), which contains nearly 1100 microRNA probes, for 326 human and 249 mouse microRNA genes, spotted in duplicates. We washed and processed the hybridised chips to detect biotin-containing transcripts with streptavidin Alexa Fluor 647 conjugate (Invitrogen, Carlsbad, CA, USA) and scanned them on a microarray scanner (4000B; Axon Instruments, Sunnyvale, CA, USA).

We analysed microarray images with GenePix Pro 6.0 (Axon Instruments). Average values of the replicate spots for every microRNA sample were background subtracted, normalised, and subjected to further analysis. Only probes for human mature microRNAs were used for analysis. We implemented quantile normalisation with the Bioconductor 1.8 package affy 1.1.2.

MicroRNAs were retained when they were present in at least 20% of samples and when they had changes of more than 1·5-fold from the gene median in at least 20% of samples. Absent calls (background-level signals on the microarray) were removed at a threshold of 4·5 ($\log_2$ scale) before statistical analysis. After the filtration, we included 237 microRNAs in further statistical analyses.

MicroRNA nomenclature is according to miRBase version 9.2.[11] The microarray dataset is deposited in ArrayExpress (experiment number E-TABM-341) according to MIAME (minimum information about a microarray experiment) guidelines.

For **ArrayExpress** see http://www.ebi.ac.uk/arrayexpress/

For the **Bioconductor 1.8 package affy 1.1.2** see http://www.bioconductor.org

See **Online** for webappendix

Statistical analysis

The panel summarises the analyses. We identified differentially expressed microRNAs with BRB-ArrayTools version 3.5.0 (Biometric Research Branch, National Cancer Institute, Bethesda, MD, USA),[29] and significance analysis of microarrays (SAM) version 3.0. The webappendix contains further descriptions of the methods used.

After filtration of microRNAs, we used the paired *t* test (level of significance, $p<0·01$) to independently analyse pairs of non-tumour mucosa and cancer samples from groups 1 and 2. We undertook class prediction with the leave-one-out cross-validation method, taking into account that samples were paired (eg, pairs of non-tumour mucosae and cancer lesions from the same patient).

We used hierarchical cluster analysis to generate a tree cluster showing the separation of every class. For hierarchical clustering, we used average linkage metrics and centred Pearson correlation of microRNAs identified between non-tumour mucosa and gastric cancer and between diffuse-type and intestinal-type gastric cancer (Cluster 3.0). For tree visualisation, we used Java Treeview version 1.1.1.

We identified microRNAs whose expression was related significantly to overall survival and disease-free survival of patients (endpoint of cancer-specific death and recurrence, respectively). We undertook univariate Cox proportional hazards regression in BRB-ArrayTools, and we judged microRNAs significant if $p<0·05$.

We used SPSS version 17.0.1 for Kaplan-Meier survival analysis and Cox proportional hazards regression. To generate survival curves, we converted continuous microRNA expression levels measured on microRNA array chips to a dichotomous variable, using the respective mean levels of expression as a threshold.[21] This procedure enabled division of samples into classes with high and low expression of microRNA. We compared survival curves by log-rank test and judged $p<0·05$ significant.

	Group 1 (n=79)	Group 2 (n=103)	p*	Total (n=182)
Age (years; mean [SD])	65·2 (9·8)	67·1 (11·6)	0·24	66·3 (10·9)
Sex			0·87	
Men	52/79 (66%)	66/102† (65%)		118/181 (65%)
Women	27/79 (34%)	36/102† (35%)		63/181 (35%)
Histological type‡			0·022	
Diffuse	53/81§ (65%)	50/103 (49%)		103/184 (56%)
Intestinal	28/81§ (35%)	53/103 (51%)		81/184 (44%)
Depth of invasion (T)‖			0·50	
T1	4/81§ (5%)	11/102† (11%)		15/183 (8%)
T2	29/81§ (36%)	38/102† (37%)		67/183 (37%)
T3	41/81§ (50%)	45/102† (44%)		86/183 (47%)
T4	7/81§ (9%)	8/102† (8%)		15/183 (8%)
Lymph-node metastasis (N)			0·028	
Negative (N0)	17/79 (22%)	37/101¶ (37%)		54/180 (30%)
Positive (N1–N3)	62/79 (78%)	64/101¶ (63%)		126/180 (70%)
Haematogenous metastasis (H, M)			0·69	
Negative	75/79 (95%)	94/102† (92%)		169/181 (93%)
Positive	4/79 (5%)	8/102† (8%)		12/181 (7%)
Peritoneal dissemination (P, CY)			<0·0001	
Negative	64/79 (81%)	12/30** (40%)		76/109 (70%)
Positive	15/79 (19%)	18/30** (60%)		33/109 (30%)
Stage††			0·13	
I	11/79 (14%)	26/102† (25%)		37/181 (21%)
II	14/79 (18%)	23/102† (23%)		37/181 (21%)
III	29/79 (37%)	27/102† (27%)		56/181 (30%)
IV	25/79 (31%)	26/102† (25%)		51/181 (28%)

Data are n (%) unless stated otherwise. *Differences between groups calculated by *t* test for age and χ^2 test for all others. †No information available for one patient. ‡Lauren's classification used for histological typing. Intestinal-type gastric cancer is almost the same as differentiated-type gastric cancer, and diffuse-type gastric cancer is almost the same as undifferentiated-type gastric cancer. §One patient had cancer in three regions. ‖Graded according to the International Union Against Cancer's TNM classification, 5th edn. ¶No information available for two patients. **No information on intraoperative cytology available for 73 patients. ††Graded according to the Japanese Classification of Gastric Cancer, 2nd English edn. Clinical stage is decided by the factors T, N, H, M, P, and CY. Stages IA and IB are regarded as stage I, and stages IIIA and IIIB as stage III.

Table 1: **Characteristics of patients and tissues**

We examined the joint effect of covariates with Cox proportional hazards regression to ascertain whether microRNAs are independent prognostic factors. We censored data for three patients who died of other diseases; data for one patient were censored before the first event (death) in overall survival and were included in the Kaplan-Meier analysis, but were removed for Cox regression analysis in overall survival.

We regarded age as a continuous covariate. T was dichotomised on the basis of absence (T1, T2) versus presence (T3, T4) of serosal invasion of tumour. Stage was dichotomised on the basis of a more than 65% 5-year survival (stages I and II) versus a less than 50% 5-year survival (stages III and IV). For all microRNAs, patients were categorised into groups with high and low expression, with respective mean levels of microRNA expression as a threshold.

We undertook univariate Cox regression to examine the effect of every clinical covariate on patient's survival. We did multivariable analysis by stepwise addition and removal of covariates found to be associated with survival in univariate models ($p<0 \cdot 10$). Conditions of the stepwise selection method were Score statistic ($p<0 \cdot 05$ for addition) and Wald statistic ($p<0 \cdot 05$ for removal). All stepwise addition models gave the same final models as did stepwise removal, and final models included only those

	p†	FDR (%)‡	Fold change	Chromosomal location	Gastric signature§	Proved targets‖	Cancer involvement¶
MicroRNAs upregulated in cancer							
miR-181d	$<1\times10^{-7}$	<0·01	2·3	19p13.12	Progression	*CDX2, GATA6, NLK*	Pancreas
miR-181a-1, miR-181a-2	$<1\times10^{-7}$	<0·01	2·2	1q31.3, 9q33.3	Progression	*HOXA11, BCL2, CD69, TRAα, PTPN11 (SHP2), PTPN22, DUSP5, DUSP6, KAT2B (PCAF), CDKN1B, CDX2, GATA6, NLK*	Breast, pancreas, liver, thyroid, uterus, brain
miR-181c	$<1\times10^{-7}$	<0·01	2·1	19p13.12	Progression	*CDX2, GATA6, NLK*	Lung, pancreas, liver, thyroid, uterus, brain
miR-181b-1, miR-181b-2	$<1\times10^{-7}$	<0·01	2·0	1q31.3, 9q33.3	Progression	*TCL1A, VSNL1, GRIA2, KAT2B (PCAF), AICDA (AID), CDX2, GATA6, NLK*	Breast, colon, pancreas, prostate, stomach, thyroid, uterus, brain, CLL
miR-21	$<1\times10^{-7}$	<0·01	2·0	17q23.2	Histotype, progression	*PTEN, TPM1, PDCD4, SERPINB5, BMPR2, BTG2, CDK6, IL6R, SOCS5, NFIB, SPRY2, RECK, TIMP3, TP63 (TP73L), DAXX, HNRNPK, TOPORS, TP53BP2, JMY, TGFBR2, TGFBR3, APAF1, PPIF, SPRY1, MTAP, SOX5, TGFB1, NCAPG, RTN4, DERL1, PLOD3, BASP1, MARCKS, IL12A, JAG1, LRRFIP1*	Breast, colon, lung, pancreas, prostate, stomach, liver, thyroid, uterus, ovary, brain, CLL, lymphoma
miR-25	$<1\times10^{-7}$	<0·01	1·7	7q22.1	Progression	*BCL2L11, KAT2B (PCAF), CDKN1C*	Pancreas, prostate, stomach, liver, thyroid, uterus, oesophagus, brain, AML
miR-92-1, miR-92-2	$<1\times10^{-7}$	<0·01	1·7	13q31.3, Xq26.2	..	*MYLIP, HIPK3, BCL2L11, VHL, ITGA5, TP63 (TP73L)*	Colon, pancreas, prostate, stomach, thyroid, CLL, AML
miR-93	$<1\times10^{-7}$	<0·01	1·6	7q22.1	Progression	*E2F1, CDKN1A, VEGFA, KAT2B (PCAF), STAT3, TP53INP1, TUSC2*	Colon, pancreas, prostate, stomach, ovary, AML
miR-17-5p	2×10^{-7}	<0·01	1·7	13q31.3	..	*E2F1, NCOA3 (AIB1), RUNX1 (AML1), RBL2, CDKN1A, PTEN, BCL2L11, TIMP1, VEGFA, HIF1A, CCND1, MAPK9, MAP3K8, PKD1, PKD2, PPARA, RBL1, STAT3, TSG101, KAT2B (PCAF), CRK, GAB1, MYCN, IRF1, NR4A3, RNF111, TP53INP1, APBB2, BRCA1, APP, RASSF2, TNFSF12, MAPK14, FN1, FNDC3A, BCL2, MEF2D, MAP3K12*	Breast, colon, lung, pancreas, prostate, stomach, bladder
miR-106a	3×10^{-7}	<0·01	1·7	Xq26.2	Progression	*RB1, RUNX1 (AML1), ARID4B (RBP1L1), MYLIP, HIPK3, CDKN1A, VEGFA, APP, IL10*	Colon, lung, pancreas, prostate, stomach, liver, AML
miR-20b	4×10^{-7}	<0·01	1·9	Xq26.2	Progression	*ARID4B (RBP1L1), MYLIP, HIPK3, CDKN1A, VEGFA*	..
miR-135a-1, miR-135a-2	7×10^{-7}	<0·01	2·1	3p21.1, 12q23.1	Progression	*APC, SMAD5, JAK2*	Colon, prostate, thyroid, uterus, AML, lymphoma
miR-425-5p	1×10^{-6}	<0·01	2·2	3p21.31	..	..	..
miR-106b	1×10^{-6}	<0·01	1·6	7q22.1	..	*E2F1, CDKN1A, VEGFA, KAT2B (PCAF), ITCH, APP, STAT3, MAPK14*	Colon, stomach, AML
miR-20a	3×10^{-6}	<0·01	1·8	13q31.3	..	*E2F1, E2F2, E2F3, TGFBR2, RUNX1 (AML1), CDKN1A, ZBTB7A (LRF), VEGFA, HIF1A, CCND1, STAT3, MYF5, APP, MAPK14, BCL2, MEF2D, MAP3K12*	Colon, pancreas, prostate, uterus, ovary, AML
miR-19b-1, miR-19b-2	5×10^{-6}	<0·01	1·7	13q31.3, Xq26.2	Histotype	*THBS1 (TSP1), MYLIP, HIPK3, SOCS1*	Prostate
miR-224	2×10^{-5}	0·02	2·2	Xq28	..	API5	Pancreas, liver, thyroid, ovary, AML
miR-18a	5×10^{-5}	0·04	1·7	13q31.3	..	*CTGF, CDKN1A, NR3C1 (GR), THBS1 (TSP1), ESR1, RUNX1 (AML1)*	Pancreas, liver, AML
miR-135b	5×10^{-5}	0·04	1·6	1q32.1	..	APC	Uterus
miR-19a	0·0008	0·5	1·5	13q31.3	Histotype, progression, prognostic	*PTEN, THBS1 (TSP1), SOCS1*	Uterus, CLL
miR-345	0·001	0·5	1·5	14q32.2	Progression	..	Prostate, thyroid
miR-191	0·002	1·0	1·3	3p21.31	..	..	Breast, colon, lung, pancreas, prostate, stomach

(Continues on next page)

	p†	FDR (%)‡	Fold change	Chromosomal location	Gastric signature§	Proved targets‖	Cancer involvement¶
(Continued from previous page)							
MicroRNAs downregulated in cancer							
miR-148a	$<1\times10^{-7}$	<0·01	0·2	7p15.2	..	*NR1I2 (PXR), DNMT3B, TGIF2*	Lung, pancreas, prostate
miR-148b	$<1\times10^{-7}$	<0·01	0·3	12q13.13	Histotype	*DNMT3B*	Colon, lung, pancreas, prostate
miR-375	$<1\times10^{-7}$	<0·01	0·3	2q35	..	*JAK2, MTPN, C1QBP, USP1, ADIPOR2, PDK1, AIFM1, RASD1, EEF1E1, GPHN, ELAVL4, CADM1, PLAG1*	Pancreas
miR-29b-1, miR-29b-2	1×10^{-6}	<0·01	0·7	7q32.3, 1q32.2	Histotype	*TCL1A, DNAJB11, SFPQ, MCL1, DNMT3A, DNMT3B, INSIG1, CAV2, BACE1, COL1A1, COL1A2, COL3A1, FBN1, ELN, YY1, PIK3R1 (p85-ALPHA), CDC42, COL4A2, COL5A3, HDAC4, TGFB3, ACVR2A, DUSP2, CTNNBIP1*	Breast, colon, lung, pancreas, prostate, thyroid, uterus, AML
miR-29c	1×10^{-5}	0·01	0·7	1q32.2	Histotype	*DNMT3A, DNMT3B, INSIG1, CAV2, COL1A1, COL1A2, COL3A1, COL4A1, COL4A2, COL15A1, SFRS13A, LAMC1, SPARC, TDG, YY1, PIK3R1 (p85-ALPHA), CDC42*	Breast, pancreas, liver, thyroid, oesophagus, nasopharyngeal
miR-152	1×10^{-5}	0·01	0·7	17q21.32	Histotype, progression	..	Pancreas
miR-218-2	2×10^{-5}	<0·01	0·6	5q34	Histotype, progression	*LAMB3, MAFG*	Lung, pancreas, prostate, stomach, liver, uterus
miR-451	6×10^{-5}	<0·01	0·4	17q11.2	..	*GATA2, ABCB1 (MDR1), MIF*	..
miR-30d	7×10^{-5}	<0·01	0·7	8q24.22	Histotype	..	Lung, pancreas, thyroid, uterus
miR-30a-5p	7×10^{-5}	0·06	0·7	6q13	..	*NOTCH1, BDNF, BECN1*	Lung, pancreas, prostate, thyroid
miR-30b	8×10^{-5}	0·06	0·7	8q24.22	Progression	..	Pancreas, prostate, uterus, lymphoma
miR-30c-1, miR-30c-2	0·0003	0·2	0·7	1p34.2, 6q13	Histotype, progression	*CTGF, RUNX1 (AML1), UBE2I*	Breast, colon, pancreas, prostate
miR-422b	0·0008	0·5	0·7	5q32	Progression	..	..

FDR=false discovery rate. AML=acute myeloid leukaemia. CLL=chronic lymphocytic leukaemia. *These microRNAs were used in the clustering of webfigure 1. †Paired class comparison. ‡1% FDR predicts that this list is 99% accurate. §Similarities in gastric cancer signature and other (histotype, progression, and prognostic) signatures. ‖Information obtained from Tarbase (http://diana.cslab.ece.ntua.gr/tarbase), miRecords (http://mirecords.umn.edu/miRecords), and previous reports.[15,23,28,34,36,39,51] ¶Information obtained from previous reports.[14-16,18-21,32]

Table 2: **Frequent differentially expressed microRNAs (gastric cancer signature)***

covariates that were associated significantly with survival (Wald statistic, $p<0·05$). We tested proportional-hazard assumption by the log-minus-log plot, and no covariate violated assumption. All p values reported are two-sided.

Role of the funding source

The sponsor had no role in study design, data collection, data analysis, data interpretation, writing of the report, or in the decision to submit for publication. The corresponding author had full access to all the data in the study and had final responsibility for the decision to submit for publication.

Results

81 gastric cancer samples (from 79 patients; one patient had cancer in three regions) were obtained at the University of Tokyo (group 1) and 103 samples were gathered at Hiroshima University (group 2) for microRNA expression profiling. Corresponding non-tumour mucosae were available for analysis for 61 cancers in group 1 and 99 in group 2. We also obtained three additional samples of non-tumour mucosa in group 1 and six in group 2, making 353 samples in total—184 cancers and 169 non-tumour mucosae.

Clinical features of patients and tumours are described in table 1 and the webappendix. Disease outcome was known for 101 patients who underwent curative surgery; 42 recurred and died of cancer within the follow-up period. The final follow-up date was Feb 25, 2007 (median follow-up 785 days [range 159–3070]). Most patients (disease stages IB–IV) were given anticancer drugs either orally or intravenously postoperatively as adjuvant chemotherapy. After disease recurrence, these individuals were given other anticancer drugs.

On microarray analysis, 35 microRNAs were expressed differentially in the paired non-tumour mucosa and cancer samples in groups 1 and 2 (table 2): 22 of these were upregulated and 13 were downregulated in cancer (designated as the gastric cancer signature). By paired class prediction, 97% of samples in group 1 and 94% in group 2 were classified correctly.

On the basis of the 35 microRNAs expressed differentially, cluster analysis with Pearson correlation of the 169 non-tumour mucosa and 184 cancer samples generated a tree showing good separation between non-tumour mucosa and cancer (page 4 of the webappendix). Despite the unpaired condition, 83% (292/353) of samples were classified correctly to non-tumour mucosa or cancer branches.

By quantitative reverse transcription-PCR (qRT-PCR), we analysed 24 pairs of samples investigated initially by microarray for miR-21 (upregulated) and miR-375 (downregulated). We compared the cancer:non-tumour mucosa expression ratio in qRT-PCR with that in the microRNA microarray. The microarray data were confirmed by qRT-PCR (page 5 of the webappendix).

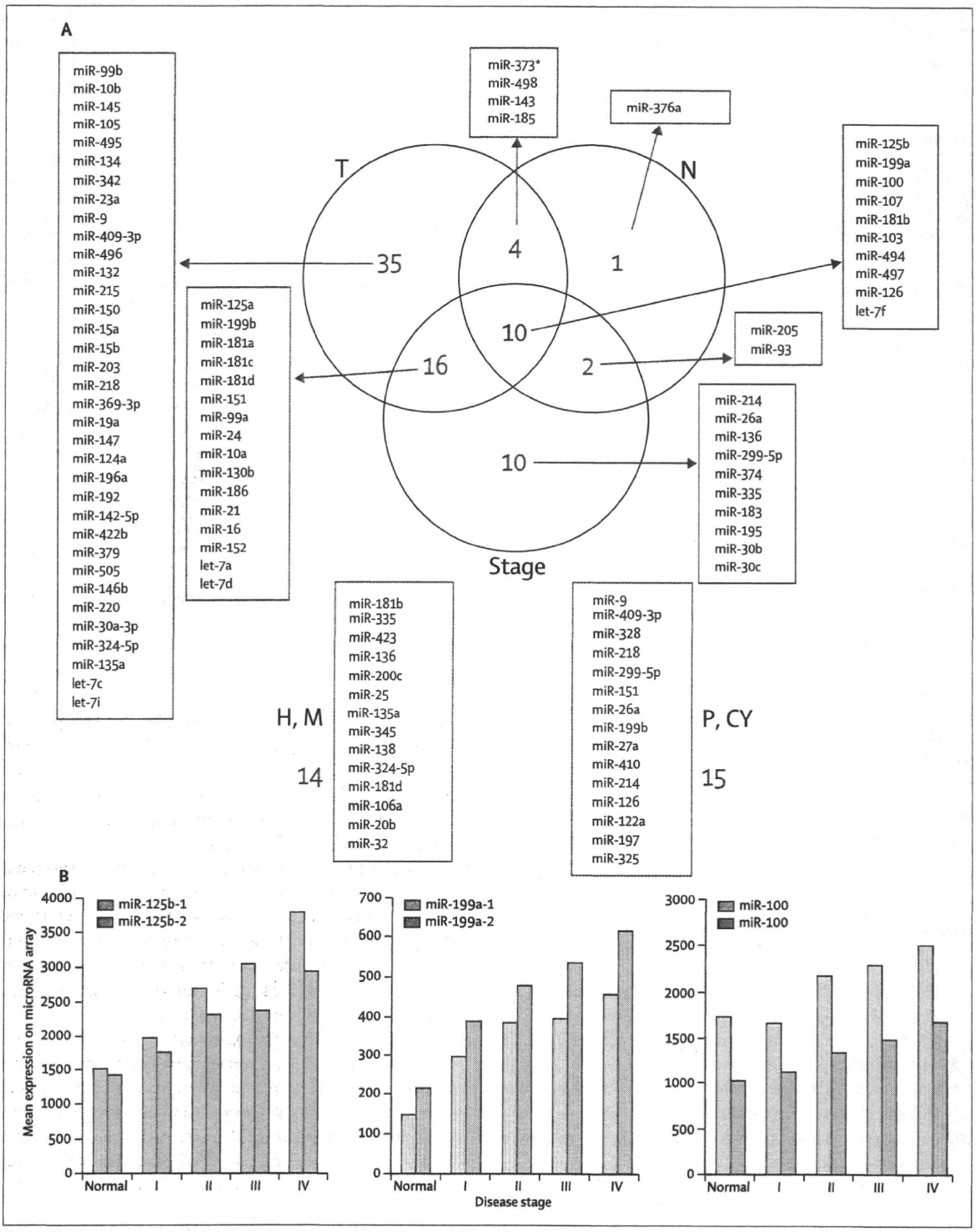

Figure 1: **MicroRNAs associated with progression of gastric cancer**

(A) Venn diagram of microRNAs related to T (depth of invasion), N (lymph-node metastasis), and stage. Listed microRNAs comprise the progression signature. Numerals indicate the number of microRNAs. Molecules corresponding to every part of the Venn diagram are shown. MicroRNAs in H and M (haematogenous metastasis) and P and CY (peritoneal dissemination) that are similar to those for T, N, or stage are shown in red. (B) Mean expression levels of miR-125b, miR-199a, and miR-100 on microRNA array according to progression in disease stage. Mean expression levels are shown as linear-scale data on microRNA array analysed with GenePix Pro 6.0; the calculation is based on the intensity (brightness) of each pixel on the microarray image. Mean expression levels of non-tumour mucosa (Normal) of group 1 are also shown. miR-125b-1 and miR-125b-2 are located on different chromosomes but the sequence of mature microRNA is the same; miR-199a-1 and miR-199a-2 are also the same. For miR-100, two probes were included on the microRNA array.

	Univariate analysis		Multivariable analysis†	
	Hazard ratio (95% CI)	p	Hazard ratio (95% CI)	p
Age	1·0 (0·9–1·0)	0·47	..	..
Sex				
Men	1·0 (reference)	0·33	..	..
Women	1·3 (0·7–2·5)		..	
Histological type				
Intestinal	1·0 (reference)	0·63	..	..
Diffuse	1·1 (0·6–2·1)		..	
T				
T1–T2	1·0 (reference)	0·001	..	..
T3–T4	3·0 (1·5–6·0)		..	
N				
Negative	1·0 (reference)	<0·0001	..	..
Positive	6·0 (2·3–15·5)		..	
Stage				
I–II	1·0 (reference)	<0·0001	1·0 (reference)	<0·0001
III–IV	5·2 (2·5–10·6)		4·3 (2·0–9·2)	
let-7g expression				
High	1·0 (reference)	0·003	1·0 (reference)	0·002
Low	2·6 (1·3–4·9)		2·9 (1·4–6·0)	
miR-214 expression				
Low	1·0 (reference)	0·007	1·0 (reference)	0·004
High	2·4 (1·2–4·5)		2·7 (1·3–5·6)	
miR-433 expression				
High	1·0 (reference)	0·015	1·0 (reference)	<0·0001
Low	2·1 (1·1–3·9)		3·4 (1·7–6·6)	
let-7e expression				
High	1·0 (reference)	0·009	..	..
Low	2·2 (1·2–4·2)		..	
let-7i expression				
High	1·0 (reference)	0·039	..	..
Low	1·9 (1·0–3·5)		..	

*One patient was censored before first event (patient's death) and these data were removed. †For the final model of multivariable analysis, stage, let-7g, miR-214, and miR-433 were included.

Table 3: **Univariate and multivariable Cox regression analysis of overall survival***

The similarity of the microRNA signature in groups 1 and 2 enabled us to merge all samples (184 cancers) into one group for further analyses. 103 diffuse-type and 81 intestinal-type specimens were used to establish whether microRNAs are differentially expressed between histological subtypes. By class comparison, 78 microRNAs were selected (false-discovery rate ≤0·42%), designated as the histotype signature.

We used the 19 most significant microRNAs (page 9 of the webappendix) in the histotype signature and undertook cluster analysis on the 184 cancer samples. These molecules were selected because they were identified also by SAM in the same order according to the absolute value of the SAM score (data not shown). Even though the histological characteristics of gastric cancer are complex (including seven histological types and mixtures of types), 74% (137/184) of tumours were distinguished successfully by the expression pattern of these 19 microRNAs (page 6 of the webappendix). Cluster analysis indicated that miR-105, miR-100, miR-125b, miR-199a, miR-99a, miR-143, miR-145, and miR-133a are upregulated in diffuse-type gastric cancer, and miR-373*, miR-498, miR-202*, and miR-494 are upregulated in intestinal-type lesions. These microRNAs are those expressed most differentially, characterising diffuse-type and intestinal-type tumours.

Next, we investigated the correlation between microRNA expression and gastric cancer progression. To identify microRNAs related to progression for every clinical feature, class comparisons were undertaken. 65 microRNAs were selected for T, 17 for N, 14 for H and M, 15 for P and CY, and 38 for stage (figure 1 A). False-discovery rate was 3·3% or less for T, 10·5% for N, 18·8% for P and CY, and 6·9% for stage. Because patients who have distant metastasis undergo surgery rarely, the sample number for positive H and M is just 12. This low number caused a reduction in power to detect microRNAs expressed differentially and a high false-discovery rate. However, six of 14 microRNAs were selected in T, N, or stage (shown in red in figure 1 A), and miR-25, miR-106a, miR-20b, miR-181b, miR-181d, and miR-135a—which were upregulated in gastric cancer relative to non-tumour mucosa—were also chosen. To identify the most important microRNAs associated with progression, we chose T and N as representative progression features and compared them with stage. Ten microRNAs—miR-125b, miR-199a, miR-100, miR-107, miR-181b, miR-103, miR-494, miR-497, miR-126, and let-7f—correlated with these variables (figure 1 A).

By SAM with rank-regression option, we selected 28 microRNAs whose expression was associated with progression from T1 to T4 and 47 microRNAs associated with progression from stage I to IV (data not shown). The q values in SAM of these microRNAs were 0% for T and 1·1% for stage. By comparison of these microRNAs with the ten identified in the previous step, we recorded miR-125b, miR-199a, and miR-100 as the most important microRNAs related to progression of gastric cancer. These three microRNAs showed increasing expression levels according to stage progression (figure 1 B).

We investigated the correlation between microRNA expression profiles and prognosis to establish the microRNAs that might signify unfavourable prognosis (independent of clinical factors). We used samples from 101 patients who underwent curative surgery and their associated prognostic information. Univariate Cox proportional hazards regression indicated that ten microRNAs (let-7c, let-7e, let-7g, let-7i, miR-19a, miR-214, miR-410, miR-433, miR-452, and miR-495) were related to overall survival of patients with gastric cancer. Kaplan-Meier survival curves were generated for every microRNA, and five (let-7e [p=0·007], let-7g [p=0·002], let-7i [p=0·038], miR-214 [p=0·005], and miR-433 [p=0·015]) were associated significantly with survival.

Table 3 shows univariate Cox proportional hazards regression analysis of overall survival relative to clinical factors. T, N, and stage were associated significantly with overall survival, as were five microRNAs. To elucidate whether these microRNAs are independent prognostic factors, multivariable analysis was done. The dichotomised expression values of these five microRNAs were not associated with clinical factors (Fisher's exact test). Because T and N were associated highly with stage by Fisher's exact test, and the same microRNAs were chosen in the final model of multivariable analysis including stage and in the final model including T and N, we showed only the stage model (table 3). In the final multivariable model, let-7g, miR-214, and miR-433 were associated with overall survival independent of clinical covariates (table 3). Patients with low expression of let-7g (hazard ratio 2·6 [95% CI 1·3–4·9]), low expression of miR-433 (2·1 [1·1–3·9]), or high expression of miR-214 (2·4 [1·2–4·5]) had poorer survival than did patients with high expression of let-7g, high expression of miR-433, or low expression of miR-214 (figure 2).

We validated the results for let-7g and miR-214 by qRT-PCR. 12 samples selected from the low-expression group showed low expression of let-7g and miR-214 by qRT-PCR, and 12 samples selected from the high-expression group showed high expression (page 7 of the webappendix). We analysed three additional specimens by qRT-PCR that were not used in microRNA array analysis because of low RNA yield. One sample with an unfavourable outcome showed high expression of miR-214 (higher than the mean of 12 samples from the high-expression group), and two with a favourable outcome showed low expression of miR-214 (lower than the mean of 12 samples from the low-expression group), consistent with our results.

We undertook the same analyses for disease-free survival in 101 patients. By univariate Cox proportional hazards regression, 12 microRNAs (let-7b, let-7c, let-7d, let-7g, miR-19a, miR-196a, miR-220, miR-373, miR-410, miR-433, miR-452, and miR-495) were related to disease-free survival of patients with gastric cancer. By log-rank analysis, six microRNAs (let-7b [p=0·001], let-7g [p=0·001], miR-19a [p=0·031], miR-410 [p=0·015], miR-433 [p=0·011], and miR-495 [p=0·035]) were related to survival. On univariate analysis, T, N, stage, and these six microRNAs were associated significantly with disease-free survival (table 4). The dichotomised expression values of six microRNAs were not associated with clinical factors (Fisher's exact test). Because T and N were associated highly with stage by Fisher's exact test, and the same microRNAs were chosen in the final model of multivariable analysis including stage and in the final model including T and N, we showed only the stage model (table 4). In the final multivariable Cox regression model, let-7b, let-7g, miR-19a, and miR-495 were associated with disease-free survival independent of clinical covariates (table 4). In

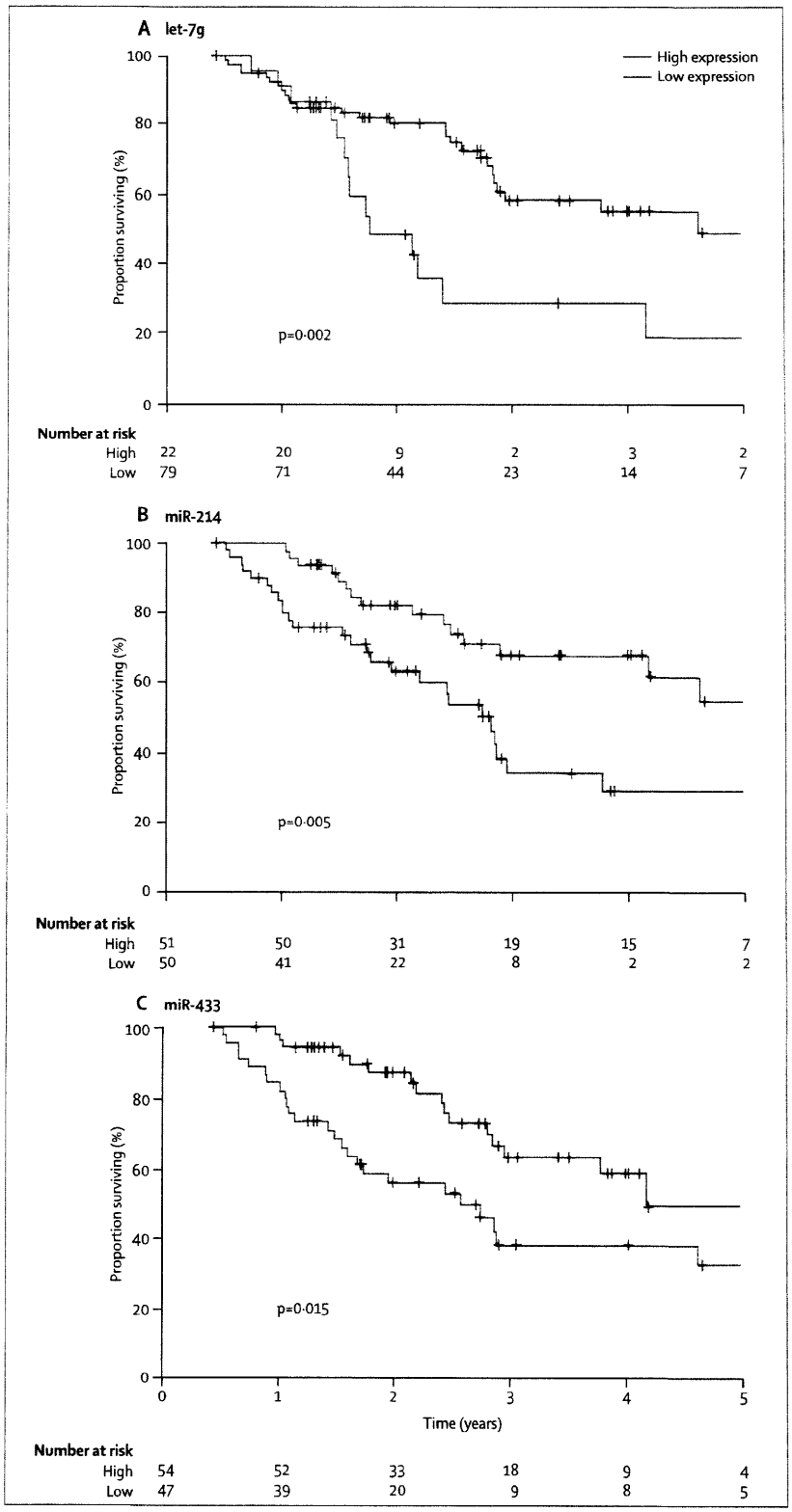

Figure 2: **Kaplan-Meier curves of independent prognostic factors for overall survival**
Curves are depicted with data for 101 patients. MicroRNA expression levels measured on the microarray were converted into discrete variables by division of samples into two classes (high and low expression), with the respective mean levels of microRNA expression as a threshold. Censored cases are shown on the curves. p values are log rank.

	Univariate analysis		Multivariable analysis†	
	Hazard ratio (95% CI)	p	Hazard ratio (95% CI)	p
Age	1·0 (0·9–1·0)	0·63	..	..
Sex				
Men	1·0 (reference)	0·31	..	..
Women	1·3 (0·7–2·5)		..	
Histological type				
Intestinal	1·0 (reference)	0·67	..	..
Diffuse	1·1 (0·6–2·1)		..	
T				
T1–T2	1·0 (reference)	0·001	..	..
T3–T4	3·1 (1·5–6·1)		..	
N				
Negative	1·0 (reference)	<0·0001	..	..
Positive	5·5 (2·1–14·2)		..	
Stage				
I–II	1·0 (reference)	<0·0001	1·0 (reference)	<0·0001
III–IV	4·5 (2·2–9·2)		5·2 (2·4–11·2)	
let-7b expression				
High	1·0 (reference)	0·003	1·0 (reference)	0·001
Low	2·7 (1·4–5·4)		3·2 (1·6–6·6)	
let-7g expression				
High	1·0 (reference)	0·002	1·0 (reference)	0·042
Low	2·7 (1·4–5·2)		2·0 (1·0–3·9)	
miR-19a expression				
High	1·0 (reference)	0·032	1·0 (reference)	<0·0001
Low	2·0 (1·0–3·6)		3·3 (1·7–6·5)	
miR-495 expression				
Low	1·0 (reference)	0·035	1·0 (reference)	0·007
High	1·9 (1·0–3·6)		2·4 (1·2–4·7)	
miR-410 expression				
Low	1·0 (reference)	0·016	..	..
High	2·2 (1·1–4·3)		..	
miR-433 expression				
High	1·0 (reference)	0·011	..	..
Low	2·1 (1·1–4·0)		..	

*No patients were censored before first event (disease recurrence). †For the final model of multivariable analysis, stage, let-7b, let-7g, miR-19a, and miR-495 were included.

Table 4: **Univariate and multivariable Cox regression analysis of disease-free survival***

both overall survival and disease-free survival, let-7g was selected as an independent prognostic factor (tables 3 and 4).

101 patients were divided into two groups by histological type (intestinal and diffuse) and multivariable Cox proportional hazards regression analysis was undertaken in the same way. The selected microRNAs remained as independent prognostic factors (table 5).

Discussion

Aberrant microRNA expression patterns have been described in various haematological and solid cancers,[14–16,20–22] and alterations in microRNA expression correlate highly with progression and prognosis of human malignant diseases.[19–24] However, profiles of microRNAs differ and need to be investigated in every type of tumour. In this study, we recorded substantial associations between differential expression of specific microRNAs and progression and prognosis of gastric cancer.

Antiapoptotic miR-21 is upregulated in various solid cancers and is related to tumour growth.[15,30] In previous work, miR-21 was overexpressed in gastric cancer and in *Helicobacter pylori*-infected gastric mucosa.[30] *H pylori* is an important pathogen for gastric cancer, and data are already starting to suggest the molecular mechanism of evolution of normal mucosa to chronic gastritis, atrophic gastritis, and intestinal metaplasia. Our sample set contained no detailed information about *H pylori* infection status because pathologists recorded histological types, depth of invasion, and status of lymph-node metastasis to decide clinical stage of cases. Non-tumour mucosae were obtained during surgery from resected stomach that seemed to be normal macroscopically. Therefore, in this study we could not investigate the correlation between microRNA expression and *H pylori* or chronic gastritis; however, we will investigate this important area in further studies.

We identified 35 differentially expressed microRNAs without use of microdissection. This procedure is difficult to adapt to some diffuse-type gastric cancers because cancer cells are localised singly. In a previous report, we analysed by microarray 20 pairs of intestinal-type gastric cancer and non-tumour mucosa samples from a white population and noted 14 upregulated and five downregulated microRNAs in cancers.[31] All the upregulated microRNAs and three of those downregulated (60%) were similar to the molecules selected in this study, meaning that our method of using bulk samples of diffuse-type gastric cancer for microarray analysis can produce correct results, although they must be validated by in-situ hybridisation. This result also means that despite patients' different ethnic backgrounds in this and our previous study, the microRNA signature is linked to general mechanisms of gastric cancer tumorigenesis.

For some of the microRNAs we identified in gastric cancer samples, several targets have already been proven experimentally. We showed previously that molecules expressed differentially in the microRNA cluster miR-106b-25 are related to gastric cancer tumorigenesis,[31] suggesting that microRNAs have important roles in gastric cancer. Although gastric cancer is histologically complex and sometimes shows transition from differentiated to undifferentiated subtypes in the same tumour (ie, mixed type), we divided samples into diffuse and intestinal types and identified microRNAs expressed differentially, characterising these histological classes. A collaborator of ours reported that the Hedgehog signal is more active in diffuse-type than intestinal-type gastric cancer,[33] and glioma-associated oncogene homologue 1 (*GLI1*), a downstream target of the Hedgehog signal, is

an in-silico target of miR-373*, which is downregulated in diffuse-type gastric cancer.

In this study, we identified microRNAs related to the progression of gastric cancer. In breast cancer, tumour invasion and metastasis are initiated by miR-10b,[24] which is one of the microRNAs associated with invasion in gastric cancer. miR-21 was selected in the progression signature of both T and stage, and it targets programmed cell death 4 (*PDCD4*) and maspin (*SERPINB5*), resulting in tumour invasion and metastasis.[24] Another group showed that miR-21 targets a tumour-suppressor gene, reversion-inducing-cysteine-rich protein with kazal motifs (*RECK*), and that knockdown of miR-21 decreased invasion and migration of gastric cancer cells significantly.[30] The microRNAs that were related most significantly to progression of gastric cancer—miR-125b, miR-199a, and miR-100—were also upregulated in pancreatic adenocarcinoma in our previous study.[21] miR-125b is reportedly related to proliferation of differentiated cells[32] and downregulated in breast cancer[14] and thyroid anaplastic carcinoma,[32] suggesting that this microRNA functions differently in gastric cancer and pancreatic adenocarcinoma. Proapoptotic *BAK1* and *TP53* are proven targets of miR-125b in prostate cancer and neuroblastoma cells, supporting the oncogenic function of miR-125b.[34,35] Upregulation of miR-199a is associated purportedly with tumour cell growth in cervical carcinoma.[36]

We identified microRNAs associated with an unfavourable outcome (independent of clinical factors) in specimens from patients treated by curative surgery and adjuvant chemotherapy. Although our findings should be validated in an independent cohort, these microRNAs might help to identify individuals who are candidates for aggressive treatment because of their expression status and who could become candidates for therapeutic targets with antagomirs[25–27] or by reconstitution with microRNA precursor sequences.[28] Three microRNAs selected in the progression analysis were not chosen for the prognostic signature partly because they were associated highly with clinical factors. The difference of the selected microRNAs between overall and disease-free survival is probably caused by the effect of chemotherapy after disease recurrence.

We chose let-7g and let-7b as independent prognostic factors. The Ras family of oncogenes is regulated by the let-7 family in lung cancer,[37,38] and the high mobility group AT-hook 2 (*HMGA2*) oncogene is also targeted by this microRNA family.[37,38] *HMGA2* is regulated negatively by the let-7 family, and high expression of this gene correlates with tumour invasiveness and is an unfavourable prognostic factor in gastric cancer.[39] Additionally, in tumour-initiating cells of breast cancer (which have stem cell-like properties), let-7 regulates self-renewal (by silencing *HRAS*) and differentiation (by silencing *HMGA2*).[24] Administration of let-7 family members inhibits growth of lung cancer in mice.[37,38] A negative regulator of hedgehog signalling, suppressor of fused (*su[fu]*), is targeted by miR-214 in the development of zebrafish,[40] and activation of hedgehog signalling is involved in gastric cancer.[32] Recently, miR-214 was reported to induce cell survival and cisplatin resistance by targeting *PTEN* in ovarian cancer.[41] miR-433 targets growth factor receptor-bound protein 2 (*GRB2*) in gastric cancer.[42]

	Hazard ratio (95% CI)	p
Disease-free survival		
Intestinal type (n=45)		
Stage, III–IV *vs* I–II*	3·2 (1·1–9·1)	0·032
let-7g expression, low *vs* high*	2·8 (1·0–7·8)	0·043
miR-19a expression, low *vs* high*	7·5 (2·3–24·6)	0·001
miR-495 expression, high *vs* low*	4·9 (1·7–14·3)	0·004
Diffuse type (n=56)		
Stage, III–IV *vs* I–II*	5·5 (1·9–15·7)	0·001
let-7b expression, low *vs* high*	2·6 (1·1–6·2)	0·031
Overall survival*		
Intestinal type (n=45)		
Stage, III–IV *vs* I–II*	5·7 (2·0–16·0)	0·001
miR-433 expression, low *vs* high*	4·4 (1·6–12·2)	0·004
Diffuse type (n=55)		
Stage, III–IV *vs* I–II*	6·3 (2·1–18·9)	0·001
miR-214 expression, high *vs* low*	2·7 (1·0–7·3)	0·048
miR-433 expression, low *vs* high*	2·4 (1·0–5·6)	0·050

*Reference group. For all microRNAs, patients were categorised into high-expression and low-expression groups with the same cutoff values of microRNA expression used in tables 3 and 4. Multivariable analysis was undertaken by stepwise addition and removal of covariates found to be associated with survival in tables 3 and 4. Only final models are shown. *In overall survival of diffuse-type gastric cancer, one patient was censored before first event (patient's death) and these data were removed.

Table 5: **Multivariable Cox regression analysis of disease-free survival and overall survival of patients with intestinal-type and diffuse-type gastric cancer**

Further studies are needed to establish whether the microRNAs we selected in this study have full potential as either biomarkers or therapeutic targets in gastric cancer. Proving new targets and other biological experiments will clarify the functions and roles of microRNAs in gastric cancer. However, we have shown already that microRNAs can meet criteria for ideal biomarkers and therapeutic targets.[22]

Contributors

All authors planned and implemented the investigation. TU, YS, MK, WY, HS, GAC, and CMC had the idea for and designed the experiments. TU, SN, NO, and KY obtained samples and clinical data. TU, HO, MS, HA, and C-gL undertook the experiments. SV, CT, SR, and TU did the statistical analysis. TU, SV, CT, GAC, and CMC wrote the report. All authors critically reviewed the manuscript and approved the final version.

Conflicts of interest

The authors declared no conflicts of interest.

Acknowledgments

We thank Karen F Phillips (Department of Scientific Publications, University of Texas MD Anderson Cancer Center) for editorial assistance. This research was supported by Program Project Grants from the National Cancer Institute (CMC) and in part by an NIH grant

1R01CA135444. GAC is supported as a fellow at the University of Texas MD Anderson Research Trust, as a fellow of the University of Texas System Regents Research Scholar, and by the Ladjevardian Regents Research Scholar Fund. SV was supported by AIRC and Regione Emilia-Romagna PRRIITT grants.

References

1 Parkin DM, Bray F, Ferlay J, Pisani P. Global cancer statistics, 2002. *CA Cancer J Clin* 2005; **55:** 74–108.

2 Hohenberger P, Gretschel S. Gastric cancer. *Lancet* 2003; **362:** 305–15.

3 Yasui W, Yokozaki H, Fujimoto J, Naka K, Kuniyasu H, Tahara E. Genetic and epigenetic alterations in multistep carcinogenesis of the stomach. *J Gastroenterol* 2000; **35:** 111–15.

4 Stock M, Otto F. Gene deregulation in gastric cancer. *Gene* 2005; **360:** 1–19.

5 Li Q-L, Ito K, Sakakura C, et al. Causal relationship between the loss of *RUNX3* expression and gastric cancer. *Cell* 2002; **109:** 113–24.

6 Jinawath N, Furukawa Y, Hasegawa S, et al. Comparison of gene-expression profiles between diffuse- and intestinal-type gastric cancers using a genome-wide cDNA microarray. *Oncogene* 2004; **23:** 6830–44.

7 Lagos-Quintana M, Rauhut R, Lendeckel W, Tuschl T. Identification of novel genes coding for small expressed RNAs. *Science* 2001; **294:** 853–58.

8 Bartel DP. MicroRNAs: genomics, biogenesis, mechanism, and function. *Cell* 2004; **116:** 281–97.

9 Krek A, Grun D, Poy MN, et al. Combinatorial microRNA target predictions. *Nat Genet* 2005; **37:** 495–500.

10 Ambros V. The functions of animal microRNAs. *Nature* 2004; **431:** 350–55.

11 Griffiths-Jones S, Grocock RJ, van Dongen S, Bateman A, Enright AJ. miRBase: microRNA sequences, targets and gene nomenclature. *Nucleic Acids Res* 2006; **34:** D140–44.

12 Bentwich I, Avniel A, Karov Y, et al. Identification of hundreds of conserved and nonconserved human microRNAs. *Nat Genet* 2005; **37:** 766–70.

13 Liu CG, Calin GA, Volinia S, Croce CM. MicroRNA expression profiling using microarrays. *Nat Protoc* 2008; **3:** 563–78.

14 Iorio MV, Ferracin M, Liu CG, et al. MicroRNA gene expression deregulation in human breast cancer. *Cancer Res* 2005; **65:** 7065–70.

15 Volinia S, Calin GA, Liu CG, et al. A microRNA expression signature of human solid tumors defines cancer gene targets. *Proc Natl Acad Sci USA* 2006; **103:** 2257–61.

16 Gramantieri L, Ferracin M, Fornari F, et al. Cyclin G1 is a target of miR-122a, a microRNA frequently down-regulated in human hepatocellular carcinoma. *Cancer Res* 2007; **67:** 6092–99.

17 Esquela-Kerscher A, Slack FJ. Oncomirs: microRNAs with a role in cancer. *Nat Rev Cancer* 2006; **6:** 259–69.

18 Calin GA, Croce CM. MicroRNA signatures in human cancers. *Nat Rev Cancer* 2006; **6:** 857–66.

19 Calin GA, Ferracin M, Cimmino A, et al. A microRNA signature associated with prognosis and progression in chronic lymphocytic leukemia. *N Engl J Med* 2005; **353:** 1793–801.

20 Yanaihara N, Caplen N, Bowman E, et al. Unique microRNA molecular profiles in lung cancer diagnosis and prognosis. *Cancer Cell* 2006; **9:** 189–98.

21 Bloomston M, Frankel WL, Petrocca F, et al. MicroRNA expression patterns to differentiate pancreatic adenocarcinoma from normal pancreas and chronic pancreatitis. *JAMA* 2007; **297:** 1901–08.

22 Schetter AJ, Leung SY, Sohn JJ, et al. MicroRNA expression profiles associated with prognosis and therapeutic outcome in colon adenocarcinoma. *JAMA* 2008; **299:** 425–36.

23 Garzon R, Volinia S, Liu CG, et al. MicroRNA signatures associated with cytogenetics and prognosis in acute myeloid leukemia. *Blood* 2008; **111:** 3183–89.

24 Nicoloso MS, Spizzo R, Shimizu M, Rossi S, Calin GA. MicroRNAs: the micro steering wheel of tumour metastases. *Nat Rev Cancer* 2009; **9:** 293–302.

25 Krützfeldt J, Rajewsky N, Braich R, et al. Silencing of microRNAs in vivo with 'antagomirs'. *Nature* 2005; **438:** 685–89.

26 Elmén J, Lindow M, Schütz S, et al. LNA-mediated microRNA silencing in non-human primates. *Nature* 2008; **452:** 896–99.

27 Akinc A, Zumbuehl A, Goldberg M, et al. A combinatorial library of lipid-like materials for delivery of RNAi therapeutics. *Nat Biotechnol* 2008; **26:** 561–69.

28 Tong AW, Nemunaitis J. Modulation of miRNA activity in human cancer: a new paradigm for cancer gene therapy? *Cancer Gene Ther* 2008; **15:** 341–55.

29 National Cancer Institute, Biometric Research Branch. BRB-ArrayTools. http://linus.nci.nih.gov/BRB-ArrayTools.html (accessed Dec 1, 2009).

30 Zhang Z, Li Z, Gao C, et al. miR-21 plays a pivotal role in gastric cancer pathogenesis and progression. *Lab Invest* 2008; **88:** 1358–66.

31 Petrocca F, Visone R, Onelli MR, et al. E2F1-regulated microRNAs impair TGFbeta-dependent cell-cycle arrest and apoptosis in gastric cancer. *Cancer Cell* 2008; **13:** 272–86.

32 Visone R, Pallante P, Vecchione A, et al. Specific microRNAs are downregulated in human thyroid anaplastic carcinomas. *Oncogene* 2007; **26:** 7590–95.

33 Fukaya M, Isohata N, Ohta H, et al. Hedgehog signal activation in gastric pit cell and in diffuse-type gastric cancer. *Gastroenterology* 2006; **131:** 14–29.

34 Shi XB, Xue L, Yang J, et al. An androgen-regulated miRNA suppresses Bak1 expression and induces androgen-independent growth of prostate cancer cells. *Proc Natl Acad Sci USA* 2007; **104:** 19983–88.

35 Le MT, Teh C, Shyh-Chang N, et al. MicroRNA-125b is a novel negative regulator of p53. *Genes Dev* 2009; **23:** 862–76.

36 Lee JW, Choi CH, Choi JJ, et al. Altered microRNA expression in cervical carcinomas. *Clin Cancer Res* 2008; **14:** 2535–42.

37 Kumar MS, Erkeland SJ, Pester RE, et al. Suppression of non-small cell lung tumor development by the let-7 microRNA family. *Proc Natl Acad Sci USA* 2008; **105:** 3903–08.

38 Esquela-Kerscher A, Trang P, Wiggins JF, et al. The let-7 microRNA reduces tumor growth in mouse models of lung cancer. *Cell Cycle* 2008; **7:** 759–64.

39 Motoyama K, Inoue H, Nakamura Y, Uetake H, Sugihara K, Mori M. Clinical significance of high mobility group A2 in human gastric cancer and its relationship to let-7 microRNA family. *Clin Cancer Res* 2008; **14:** 2334–40.

40 Flynt AS, Li N, Thatcher EJ, Solnica-Krezel L, Patton JG. Zebrafish miR-214 modulates Hedgehog signaling to specify muscle cell fate. *Nat Genet* 2007; **39:** 259–63.

41 Yang H, Kong W, He L, et al. MicroRNA expression profiling in human ovarian cancer: miR-214 induces cell survival and cisplatin resistance by targeting PTEN. *Cancer Res* 2008; **68:** 425–33.

42 Luo H, Zhang H, Zhang Z, et al. Down-regulated miR-9 and miR-433 in human gastric carcinoma. *J Exp Clin Cancer Res* 2009; **28:** 82.

Oncogene (2010) 29, 2036–2046

www.nature.com/onc

ORIGINAL ARTICLE

Wnt5a signaling is involved in the aggressiveness of prostate cancer and expression of metalloproteinase

H Yamamoto[1,2], N Oue[3], A Sato[4], Y Hasegawa[5], H Yamamoto[4], A Matsubara[5], W Yasui[3] and A Kikuchi[4]

[1]Department of Biochemistry, Graduate School of Biomedical Sciences, Hiroshima University, Hiroshima, Japan; [2]Department of Surgery, Graduate School of Biomedical Sciences, Hiroshima University, Hiroshima, Japan; [3]Department of Molecular Pathology, Graduate School of Biomedical Sciences, Hiroshima University, Hiroshima, Japan; [4]Department of Molecular Biology and Biochemistry, Graduate School of Medicine, Faculty of Medicine, Osaka University, Suita, Japan and [5]Department of Urology, Graduate School of Biomedical Sciences, Hiroshima University, Hiroshima, Japan

Wnt5a is a representative ligand that activates the β-catenin-independent pathway in Wnt signaling. Although it has been reported that abnormal activation of the Wnt/β-catenin-dependent pathway is often observed in human prostate cancer, the involvement of the β-catenin-independent pathway in this cancer is unclear. Abnormal expression of Wnt5a and β-catenin was observed in 27 (28%) and 49 (50%) of 98 prostate cancer cases, respectively, by immunohistochemical analyses. Simultaneous expression of Wnt5a and β-catenin was observed in only five cases, suggesting their exclusive expression. The positive detection of Wnt5a was correlated with high Gleason scores and biochemical relapse of prostate cancer, but that of β-catenin was not. Knockdown and overexpression of Wnt5a in human prostate cancer cell lines reduced and stimulated, respectively, their invasion activities, and the invasion activity required Frizzled2 and Ror2 as Wnt receptors. Wnt5a activated Jun-N-terminal kinase through protein kinase D (PKD) and the inhibition of PKD suppressed Wnt5a-dependent cell migration and invasion. In addition, Wnt5a induced the expression of metalloproteinase-1 through the recruitment of JunD to its promoter region. These results suggest that Wnt5a promotes the aggressiveness of prostate cancer and that its expression is involved in relapse after prostatectomy.
Oncogene (2010) **29**, 2036–2046; doi:10.1038/onc.2009.496; published online 18 January 2010

Keywords: Wnt5a; prostate cancer; Gleason score; invasion; MMP-1

Introduction

Prostate cancer (PCa) is an increasingly prevalent cancer in men, which develops and progresses under the influence of androgenic steroids (Jemal *et al.*, 2008). PCa screening by assessing serum prostate-specific antigen (PSA) level has led to increased detection of early-stage PCa that can be cured by radical prostatectomy or radiation therapy. Although overall cancer control rates are high for clinically localized diseases, 20–30% of patients will experience recurrence manifested initially as a rising PSA level without clinical or radiographic metastasis (Han *et al.*, 2003). This biochemical relapse is indicative of the presence of prostate tissue and is assumed to represent cancer. Many patients with biochemical relapse have indolent disease that grows slowly and requires no treatment but some will have rapid progression. A critical issue for patients is determination of whether rising PSA represents local or systemic disease, as the former may be cured by salvage radiotherapy and the latter requires hormone therapy. High risk of recurrence is defined according to preoperative PSA level (>20 ng/ml), biopsy Gleason score (≥8) and the 1992 American Joint Committee on Cancer clinical T stage (≥T2c) (Partin *et al.*, 1997; D'Amico *et al.*, 2000). These factors are helpful but not perfect due to significant clinical heterogeneity. Identifying molecules that are expressed in clinically localized PCa but associated with PCa invasion and metastasis might significantly improve the prognostic capabilities and management of patients with PCa after a curative approach.

The accumulation of cytoplasmic and nuclear β-catenin has been documented in many malignancies, including breast, gastric, colon, esophageal, hepatic, pancreatic, thyroid, cerebellar and skin carcinoma (Polakis, 2000; Kikuchi, 2003). In PCa, abnormal accumulation of β-catenin has been detected in 20–50% of tumors, and high levels of β-catenin expression are associated with advanced, metastatic and hormone-refractory PCa (Yardy and Brewster, 2005). Although β-catenin was originally identified as a cadherin-binding protein, it is known to be a key molecule in the Wnt signaling pathway. Wnt proteins are a large family of cysteine-rich secreted molecules that exhibit unique expression patterns and distinct functions in development (Logan and Nusse, 2004). The well-established intracellular signaling pathway activated by Wnt proteins is a β-catenin-dependent signaling pathway that is

Correspondence: Dr A Kikuchi, Department of Molecular Biology and Biochemistry, Graduate School of Medicine, Faculty of Medicine, Osaka University, 2-2, Yamadaoka, Suita 565-0871, Japan.
E-mail: akikuchi@molbiobc.med.osaka-u.ac.jp
Received 4 August 2009; revised 4 November 2009; accepted 8 December 2009; published online 18 January 2010

highly conserved among species (Logan and Nusse, 2004; Kikuchi *et al.*, 2009). When Wnt acts on its cell-surface receptor, which consists of Frizzled and low-density lipoprotein receptor-related protein 5/6, cytoplasmic β-catenin is stabilized by release from the Axin complex. The accumulated β-catenin is translocated to the nucleus, where it binds to the transcription factor T-cell factor/lymphoid enhancer factor and thereby stimulates the expression of various genes (Hurlstone and Clevers, 2002). At least 19 Wnt members have been shown to be present in mammals to date, and some Wnts, including Wnt1, Wnt3a and Wnt7a, activate the β-catenin pathway. In addition to T-cell factor/lymphoid enhancer factor, β-catenin binds to androgen receptor, and these Wnt ligands also increase androgen receptor-mediated transcription even in the absence of androgen ligands (Verras *et al.*, 2004). Therefore, activation of the β-catenin pathway appears to be involved in the initiation and progression of PCa as shown in other tumors.

Another class of Wnts, including Wnt2, Wnt4, Wnt5a, Wnt5b, Wnt6 and Wnt11, activates a β-catenin-independent pathway that primarily modulates cell movement and polarity (Veeman *et al.*, 2003). This pathway is known to activate several protein kinases including Ca^{2+}/calmodulin-dependent protein kinase II, protein kinase C (PKC), c-jun N-terminal kinase (JNK) and Rho-associated kinase. Wnt5a is a representative of the Wnt proteins that activate the β-catenin-independent pathway, which includes multiple pathways, and Wnt5a activates distinct routes (Veeman *et al.*, 2003; Kurayoshi *et al.*, 2007; Kikuchi and Yamamoto, 2008). It has been shown that Wnt5a stimulates migration in some cancer cells and that its expression is correlated with the aggressiveness of melanoma, breast cancer, lung cancer and gastric cancer (Weeraratna *et al.*, 2002; Veeman *et al.*, 2003; Huang *et al.*, 2005; Kurayoshi *et al.*, 2006; Pukrop *et al.*, 2006; Kikuchi and Yamamoto, 2008; Yamamoto *et al.*, 2009), suggesting that Wnt5a has oncogenic properties. Other reports indicate that Wnt5a acts as a tumor suppressor based on the finding that Wnt5a has an ability to inhibit proliferation, migration and invasiveness in thyroid tumor and colorectal cancer cell lines (Dejmek *et al.*, 2005; Kremenevskaja *et al.*, 2005). Although the β-catenin-independent pathway activated by Wnt5a is also involved in tumorigenesis, the relationship between the expression of Wnt5a and PCa is not well understood. This study showed that a high expression level of Wnt5a significantly correlates with biochemical relapse of clinically localized PCa cases treated with radical prostatectomy. It was also shown that Wnt5a promotes invasion activities of PCa cells at least through the activation of JNK and the expression of matrix metalloproteinase-1 (MMP-1).

Results

Immunohistochemical analysis of Wnt5a in PCa tissues

Preceding immunohistochemical studies showed that approximately 30% of 237 gastric cancer cases exhibit high expression levels of Wnt5a (Kurayoshi *et al.*, 2006). Using the same antibody, we examined the expression of Wnt5a in PCa. In adjacent non-neoplastic prostate tissue including glandular hyperplasia, weak or no staining of Wnt5a was observed in epithelial and stromal cells (Figure 1a). However, PCa tissue showed stronger and more extensive staining than corresponding non-neoplastic mucosa (Figure 1a). In the majority of PCa cases containing Wnt5a-positive tumor cells, more than 50% of the tumor cells showed cytoplasmic staining for Wnt5a. Of 98 PCa cases, 27 (28%) were positive for Wnt5a. In these PCa cases, no tendency of strong staining for Wnt5a at the invasive front was observed. The relationship between Wnt5a staining and clinicopathological characteristics was analyzed. Wnt5a positivity was found more frequently in PCa showing a Gleason score $\geqslant 8$ (12/24, 50%) than in PCa showing a Gleason score $\leqslant 7$ (15/74, 20%, $P=0.0079$, Fisher's exact test) (Supplementary Table S1). Therefore, the expression of Wnt5a may be associated with the aggressiveness of PCa. However, Wnt5a staining did not correlate with age, pT classification or preoperative PSA concentration (Supplementary Table S1).

An immunohistochemical analysis of β-catenin expression in PCa was also performed. Although β-catenin was usually detected at the cell membranes, cytosomal or nuclear accumulation of β-catenin was observed in 49 (50%) of 98 PCa cases (Supplementary Table S2). However, β-catenin staining in cytoplasm and nucleus did not correlate with age, pT classification, Gleason score or preoperative PSA concentration (Supplementary Table S2). These results suggested that the abnormal expression of β-catenin may be involved in the initiation of PCa but not in the aggressiveness of the tumor. The relationship between the expression of Wnt5a and β-catenin in PCa was analyzed further. Wnt5a positivity was found more frequently in cytosomal or nuclear β-catenin-negative cases (22/49, 45%) than in cytosomal or nuclear β-catenin-positive cases (5/49, 10%, $P=0.0002$, Fisher's exact test) (Supplementary Table S1). In the five PCa cases positive for both Wnt5a and cytosomal or nuclear β-catenin, there was a tendency that Wnt5a-positive cancer cells do not show cytosomal or nuclear accumulation of β-catenin (Figure 1b). These findings suggested that Wnt5a and cytosomal and nuclear β-catenin are expressed in an exclusive pattern in PCa.

Relapse of patients with PCa expressing Wnt5a

Next, the relationship between Wnt5a immunostaining and relapse in PCa was examined. Univariate analysis revealed that the expression of Wnt5a ($P=0.0045$, log-rank test) decreases the ratios of relapse-free survival in patients as well as high Gleason score ($P<0.0001$) and high preoperative PSA concentration ($P=0.0167$) (Figure 2a), whereas cytosomal or nuclear accumulation of β-catenin, age and pT classification did not correlate with relapse (Figure 2b). A Cox proportional hazards multivariate model was used to examine the relationship between clinicopathological factors, expression of Wnt5a and β-catenin, and relapse-free survival. Multi-

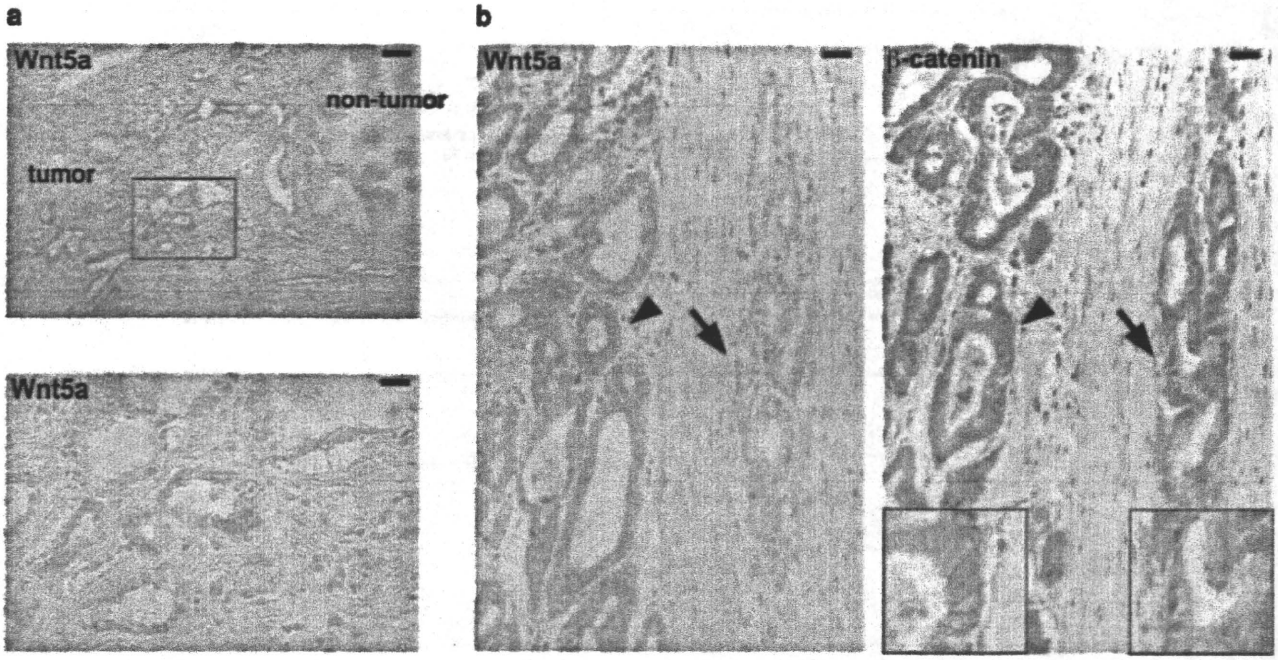

Figure 1 Immunohistochemical analyses of Wnt5a and β-catenin in prostate cancer (PCa). (**a**) Top panel, expression levels of Wnt5a in nontumor and tumor regions were compared. Bar, 50 μm. Bottom panel, high-magnification image of the fields indicated by the box in the upper panel. The tumor regions were enlarged. Bar, 12 μm. (**b**) A sample of PCa was stained with anti-Wnt5a (left panel) and anti-β-catenin (right panel) antibodies. Bars, 25 μm. Arrowheads indicate Wnt5a-positive and cytosomal or nuclear β-catenin-negative PCa cells. Arrows indicate Wnt5a-negative and cytosomal or nuclear β-catenin-positive PCa cells. Insets, high-magnification images of the fields indicated by the arrow and arrowhead in the right panel.

variate analysis indicated that Wnt5a staining, Gleason score and preoperative PSA concentration are independent predictors of relapse of PCa, but cytosomal or nuclear β-catenin staining, age and pT classification are not (Table 1). These results suggested that Wnt5a expression contributes directly to the malignant potential of PCa.

Involvement of Wnt5a in migration and invasion of PCa cells

To understand the relationship between the expression of Wnt5a and aggressiveness of PCa, we examined the expression levels of various Wnts in PCa cells (Figure 3a). DU145 and PC3 cells are androgen-independent PCa cells and LNCap cells are androgen-dependent PCa cells. *Wnt5a* mRNA was highly expressed in DU145 and LNCap cells, but PC3 cells showed a low expression level. mRNA expression of *Wnt4* was observed in all cell lines. *Wnt5b* mRNA was detected in DU145 but not in LNCap and PC3 cells. Neither *Wnt3a* nor *Wnt11* mRNA was detected in these cells. Wnt5a siRNA reduced the mRNA level of *Wnt5a* in LNCap cells and suppressed migration activity in transwell assays using a Boyden chamber (Figure 3b, Supplementary Figure S1). Knockdown of Wnt5a in DU145 cells also decreased cell migration (Figure 3c), but knockdown of Wnt5b did not (data not shown). Wnt7a siRNA did not affect cell migration of LNCap and DU145 cells (Figures 3b and c, Supplementary Figure S1). Migration activity in Wnt4-knockdwon cells was decreased to about 70% of control cell (Figure 3c). Wnt4 has been reported to activate both the β-catenin-dependent and β-catenin-independent pathways (Bernard and Harley, 2007), but the role of Wnt4 in cell migration is not well understood. Therefore, we did not study the role of Wnt4 in migration of PCa cells further. It is known that DU145 and PC3 cells, but not LNCap cells, have invasion activities. Whereas control DU145 cells invaded the Matrigel, Wnt5a knockdown cells were less invasive (Figure 3c). Transient overexpression of Wnt5a enhanced the invasion activities of PC3 cells, but that of Wnt5a CA, which is an inactive form of Wnt5a generated by mutating Cys104 to Ala (Kurayoshi *et al*., 2007), did not (Figure 3d).

Secreted Frizzled-related protein 2 (sFRP2) binds to Wnt proteins and acts as a negative regulator of Wnt signaling (Kawano and Kypta, 2003). DU145 cells were allowed to migrate in scratch-wound cultures, resulting in wound closure after 24 h, and the migration of DU145 cells in scratch-wound cultures was inhibited by the addition of sFRP2 conditioned medium (CM) (Figure 3e). Furthermore, an anti-Wnt5a antibody suppressed the migration of DU145 cells in scratch-wound cultures (Figure 3f). Taken together, these results indicated that Wnt5a stimulates cell migration and invasion in PCa cells.

Mechanism of Wnt5a-induced invasion by PCa cells

The mechanism by which Wnt5a induces invasion of DU145 and PC3 cells was examined as an *in vitro* model

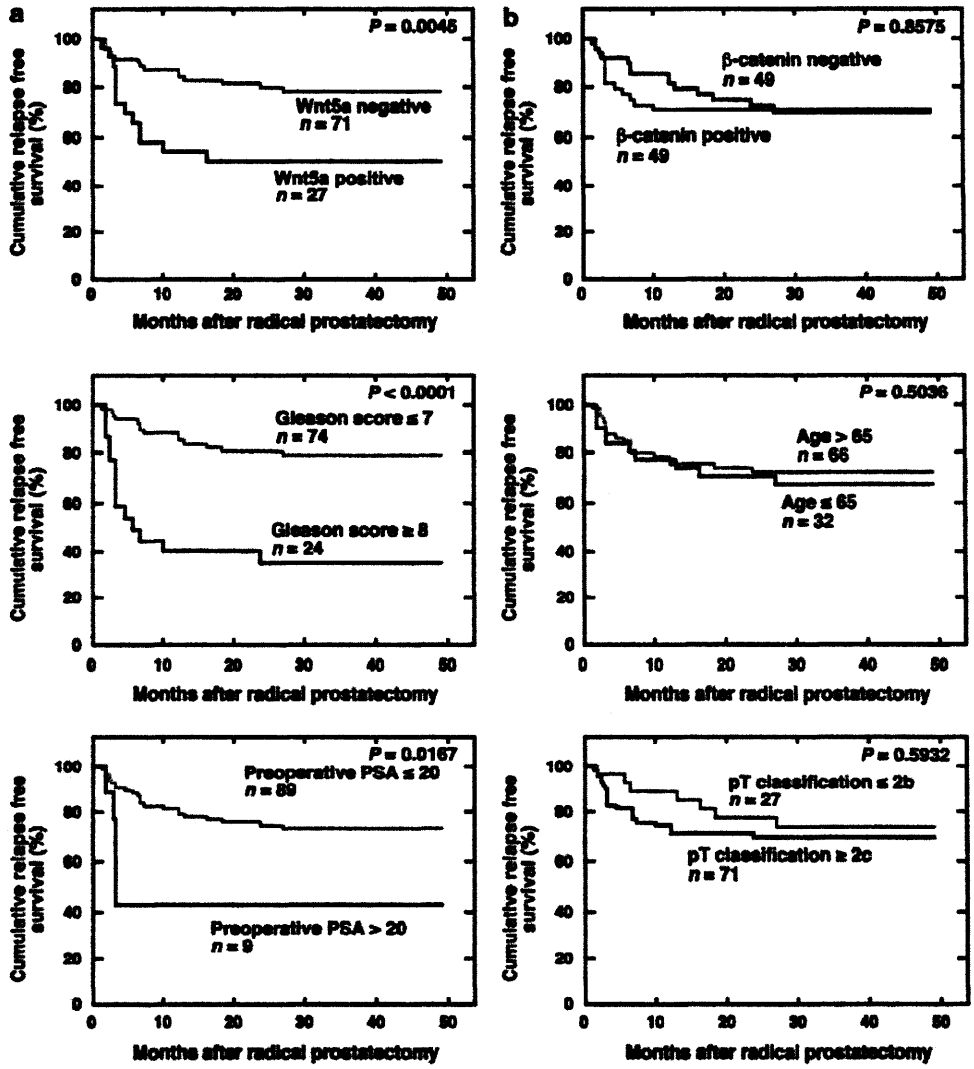

Figure 2 Relapse-free survival of patients with prostate cancer (PCa) expressing Wnt5a or β-catenin. (**a**) Kaplan–Meier curves of patients with PCa with Wnt5a-negative or Wnt5a-positive PCa (upper panel), with low Gleason score (≤7) or high Gleason score (≥8) PCa (middle panel), and with low preoperative prostate-specific antigen (PSA) concentration (≤20 ng/ml) or high preoperative PSA concentration (>20 ng/ml) (lower panel). (**b**) Kaplan–Meier curves of patients with PCa with or without β-catenin expression in the cytoplasm and nucleus (upper panel), with younger (≤65) or older (>65) age (middle panel) and with low pT classification (≤2b) or high pT classification (≥2c) PCa (lower panel).

of invasive PCa cells. Frizzled (Fz) family members are known to function as Wnt receptors (Wang *et al.*, 2006). Fz2, Fz6 and Fz7 were expressed highly in DU145 cells compared with other Fzs (Supplementary Figure S2a). Wnt5a bound to Fz2, Fz5 and Fz8 but not to Fz6 and Fz7 (Sato *et al.*, 2010) (data not shown), and Ror2, a single transmembrane protein, is known to function as a Wnt5a receptor (Oishi *et al.*, 2003). To examine which receptor(s) are involved in cell migration of DU145 cells, we depleted Wnt receptors by siRNA (Supplementary Figure S2b). Knockdown of Fz2 and Ror2 but not Fz6 reduced cell invasion by DU145 cells significantly (Figure 4a). Knockdown of Fz7 showed a tendency to decrease cell invasion, but the difference was not statistically significant (Figure 4a). Wnt5a induced the phosphorylation of protein kinase D (PKD)/PKCμ in DU145 cells (Figure 4b). PKD is a protein kinase, which not only is a direct target of diacylglycerol but also lies downstream of novel PKCs (Rozengurt *et al.*, 2005). Therefore, these results suggested that Wnt5a activates novel PKCs. Staurosporine, a PKC inhibitor, indeed suppressed Wnt5a-dependent migration and invasion activities of DU145 cells (Figure 4b). Furthermore, Gö6976, an inhibitor that is relatively specific for PKD, suppressed Wnt5a-dependent migration and invasion activities of DU145 cells (Figure 4b). These results suggested that PKD activation by Wnt5a probably through the activation of novel PKCs is involved in Wnt5a-dependent migration and invasion. In addition, Wnt5a activated small G protein Rac, which has a role in cell migration (Figure 4c).

It has been reported that many genes associated with aggressive behavior, including Wnt5a and MMP-9, were increased in androgen-independent metastatic tumors

Table 1 Multivariate analysis of factors influencing relapse-free survival

	Hazard ratio (95% CI)	χ^2	P-*value*
Wnt5a staining			
Negative	1 (Reference)	3.907	0.0312
Positive	2.451 (1.007–5.960)		
Cytosomal or nuclear β-catenin staining			
Negative	1 (Reference)	1.681	0.1947
Positive	1.782 (0.744–4.265)		
Age			
⩽65	1 (Reference)	0.101	0.7507
>65	1.138 (0.513–2.525)		
pT classification			
⩽2b	1 (Reference)	0.161	0.6882
⩾2c	1.215 (0.469–3.148)		
Gleason score			
⩽7	1 (Reference)	10.976	0.0009
⩾8	3.912 (1.745–8.769)		
Preoperative PSA concentration			
⩽20	1 (Reference)	4.574	0.0325
>20	3.176 (1.101–9.161)		

Abbreviations: CI, confidence interval; PSA, prostate-specific antigen.

and that MMP-1 is involved in invasion by DU145 cells (Stanbrough *et al.*, 2006; Zeng *et al.*, 2006). The stimulation of DU145 cells with Wnt5a increased the expression of *MMP-1* (collagenase) mRNA but not those of *MMP-2* (gelatinase A), *MMP-3* (stromyelysin-1) or *MMP-9* (gelatinase B) mRNA, and knockdown of Wnt5a decreased the levels of *MMP-1* mRNA (Figure 5a). Consistent with these results, Wnt5a increased the protein levels of MMP-1 (Figure 5a). As shown in transient expression of Wnt5a in PC3 cells, the invasion activities of PC3 cells were also enhanced by stable expression of Wnt5a, and knockdown of MMP-1 suppressed the invasion activities (Figure 5a). To evaluate the role of Wnt5a on *MMP-1* promoter activity, we transfected the *MMP-1* 5′-flanking region containing two activator protein-1 (AP-1) sites (−517/+60) with *luciferase* gene into PC3 cells (Figure 5b). Wnt5a increased the promoter activity (Figure 5b). It was reported that the proximal AP-1 site at −72 is necessary for the phorbol ester-induced expression of MMP-1 (Hall *et al.*, 2003). The basal reporter gene activity was decreased by introducing mutations in this area (*AP-1 mut*), and Wnt5a did not stimulate it (Figure 5b). Consistent with these results, Wnt5a indeed induced the phosphorylation of JNK at Thr183 and Tyr185, which indicates the activation of JNK, in DU145 cells (Figure 5c). In addition, Gö6976 suppressed Wnt5a-dependent JNK activation (Figure 5c), suggesting Wnt5a activates JNK through PKD. c-Jun or JunD has been shown to bind to the AP-1 site in the promoter region of *MMP-1* in MKN45 and U937 cells (Doyle *et al.*, 1997; Wu *et al.*, 2006). In a chromatin immunoprecipitation assay, *MMP-1* promoter occupancy of JunD was decreased in DU145/Wnt5a knockdown cells compared with DU145/control cells (Figure 5d). Furthermore, Gö6976 interfered the binding of JunD to *MMP-1* promoter, but knockdown of Rac did not affect the Wnt5a-induced binding of JunD and *MMP-1* promoter (Figure 5d). Taken together, these results suggested that Fz2 and Ror2 function as Wnt5a receptors in this signaling of PCa cells and that PKD and JNK mediate Wnt5a-dependent expression of MMP-1 through the recruitment of JunD to the AP-1 site of the *MMP-1* promoter.

Discussion

Clinical relevance of Wnt5a expression in PCa

PCa is the most commonly diagnosed malignancy, and its incidence is rising in many countries (Hsing *et al.*, 2000; Jemal *et al.*, 2008). The present results showed that the expression of Wnt5a is correlated with a prostatectomy Gleason score ⩾8. Gleason score is the most frequently used grading system for PCa and is a powerful prognostic indicator (Gleason and Mellinger, 1974). It has also been reported that prostatectomy Gleason score is a predictor of distant metastasis (Pound *et al.*, 1999). When the Gleason score was ⩾8, the probability of distant metastasis was >65% at 5 years. In the present cases, patients with a Gleason score ⩾8 indeed showed a significantly higher risk of biochemical relapse. Furthermore, multivariate analyses showed that the expression of Wnt5a is an independent predictor of biochemical relapse, along with prostatectomy Gleason score and preoperative PSA concentration, indicating that Wnt5a might be a good indicator of the recurrence of PCa. Biochemical relapse indicates the presence of PCa, which may have already migrated to distant sites when the prostatectomy was performed. PCa cells positive for Wnt5a expression could have an ability to invade. Knockdown and overexpression of Wnt5a in PCa cells indeed inhibited and activated, respectively, their migration and invasion activities. Taken together with the observations that sFRP2 and anti-Wnt5a antibody inhibited migration of PCa cells, it is conceivable that Wnt5a is a candidate molecular target of therapy for PCa.

It has been reported that high levels of β-catenin are associated with aggressiveness in PCa (Yardy and Brewster, 2005). Among the current 98 cases, PCa abnormally expressing both Wnt5a and β-catenin was observed in only 5 cases. This is similar to the situation in cases of gastric cancer (Kurayoshi *et al.*, 2006). At present the reason why the expression of Wnt5a and β-catenin is mutually exclusive is not known.

Mechanism by which Wnt5a promotes aggressiveness of PCa

How is Wnt5a involved in the aggressiveness of PCa? Wnt5a increased *MMP-1* mRNA and protein levels in PCa cells, but it did not induce the expression of *MMP-2*, *MMP-3* and *MMP-9* mRNAs. MMPs are zinc-containing endopeptidases that degrade extracellular matrix components and are associated with cancer cell invasion and metastasis (Egeblad and Werb, 2002). It was suggested that upregulation of MMP-1 is an

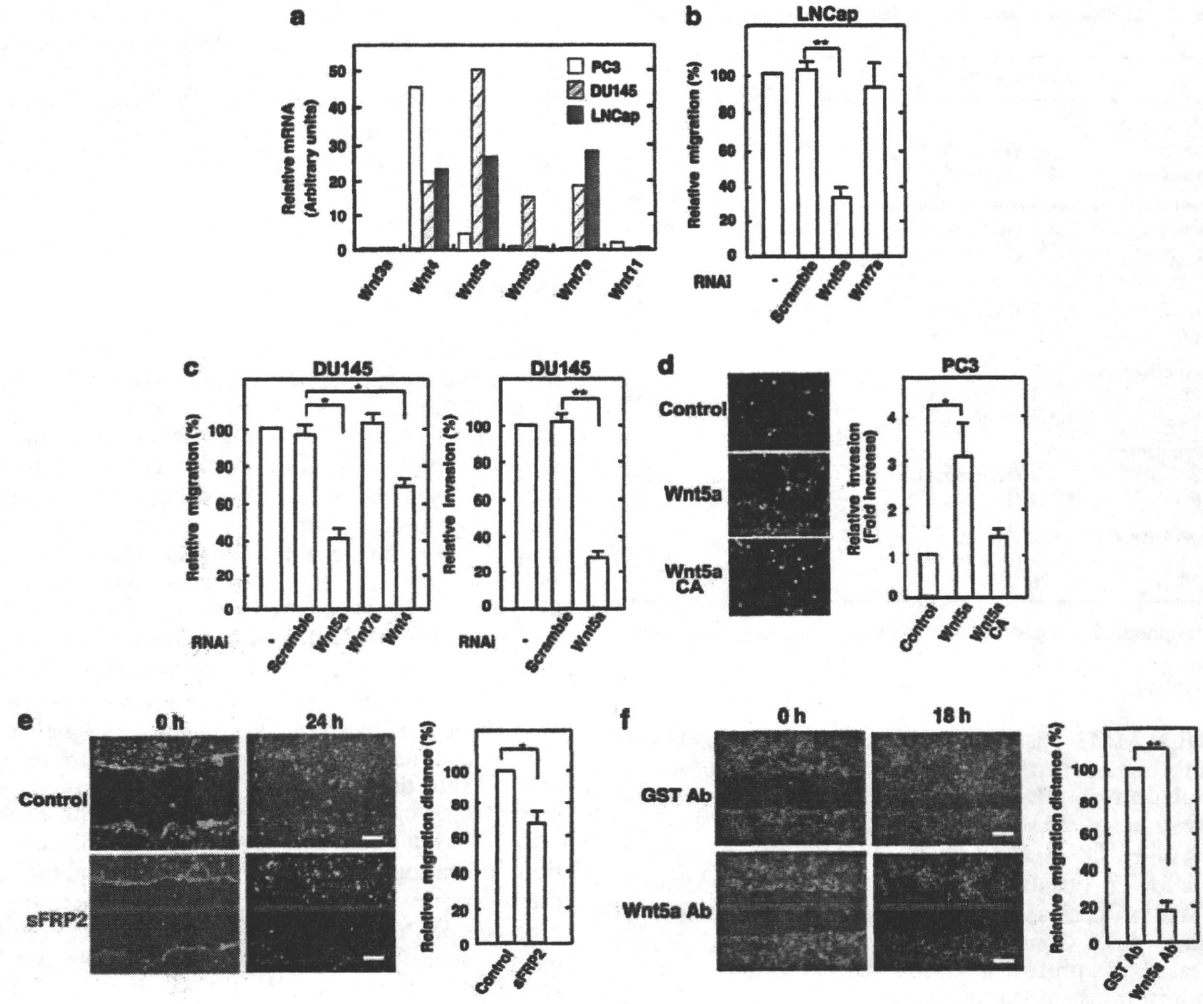

Figure 3 Wnt5a is involved in migration and invasion of prostate cancer (PCa) cells. (**a**) The mRNA levels of various Wnts in PC3, DU145 and LNCap cells were quantified by quantitative reverse transcription (RT)–PCR. (b) LNCap cells transfected with *scrambled* (control), *Wnt5a* or *Wnt7a* siRNA were placed in transwell chambers for a migration assay toward fibronectin. In three independent fields, 130 ± 7 untransfected cells transmigrated. Relative migration activities were expressed as percentages for the migration of untransfected cells. The results shown are means ± s.e. from three independent experiments. $^{**}P<0.01$. (**c**) DU145 cells transfected with *scrambled*, *Wnt5a*, *Wnt7a* or *Wnt4* siRNA were placed in noncoated (left panel) or Matrigel-coated (right panel) transwell chambers for migration and invasion assays. In three independent fields, 189 ± 11 untransfected cells transmigrated and 34 ± 6 untransfected cells invaded. Relative migration and invasion activities were expressed as percentages for the migration and invasion of untransfected cells. $^{*}P<0.05$; $^{**}P<0.01$. (**d**) Left panel, PC3 cells transfected with pPGK empty vector (control), pPGK/wild-type Wnt5a (Wnt5a) or pPGK/Wnt5a^{C104A} (Wnt5a CA) were placed in Matrigel-coated transwell chambers for an invasion assay. Right panel, in eight independent fields, 22 ± 12 of PC3 cells transfected with empty vector invaded. Relative invasion activities were expressed as fold increases compared with the invasion of transfectants with empty vector. $^{*}P<0.05$. (**e**) Control or secreted Frizzled-related protein 2 (sFRP2) conditioned medium (CM) was added to DU145 cells and then the cells were wounded. The culture was further continued for 24 h. Bars, 200 μm. Right graph, migration distances were measured and expressed as percentages of the migration in the presence of control CM. $^{*}P<0.05$. (**f**) DU145 cells incubated with anti-glutathione *S*-transferase (GST) or anti-Wnt5a antibody (10 μg/ml) were wounded. The culture was continued for 18 h. Bars, 200 μm. Right graph, migration distances were measured and expressed as percentages of the migration in the presence of anti-GST antibody. $^{**}P<0.01$.

important factor in the aggressiveness of PCa and bone marrow metastasis (Hart *et al.*, 2002). This study showed that knockdown of MMP-1 indeed suppressed Wnt5a-dpendent invasion of PC3 cells *in vitro*.

Although how MMP-1 is overexpressed in PCa is not clear, one report showed that a pathway involving FAK, PI3K and PKCδ activated by engagement of integrin α5β1 with fibronectin regulates the expression of MMP-1 in DU145 cells (Zeng *et al.*, 2006). It was also shown previously that Wnt5a induces the expression of MMP-1 in endothelial cells although the mechanism was not known (Masckauchan *et al.*, 2006). This study found that Wnt5a induces the phosphorylation of PKD/PKCμ, which is a direct target of novel PKCs (PKCδ, PKCε, PKCη and PKCθ), and activates JNK. Furthermore, it was shown that Wnt5a signaling recruits JunD to the AP-1 site of the *MMP-1* promoter region. These results were consistent with the previous observations

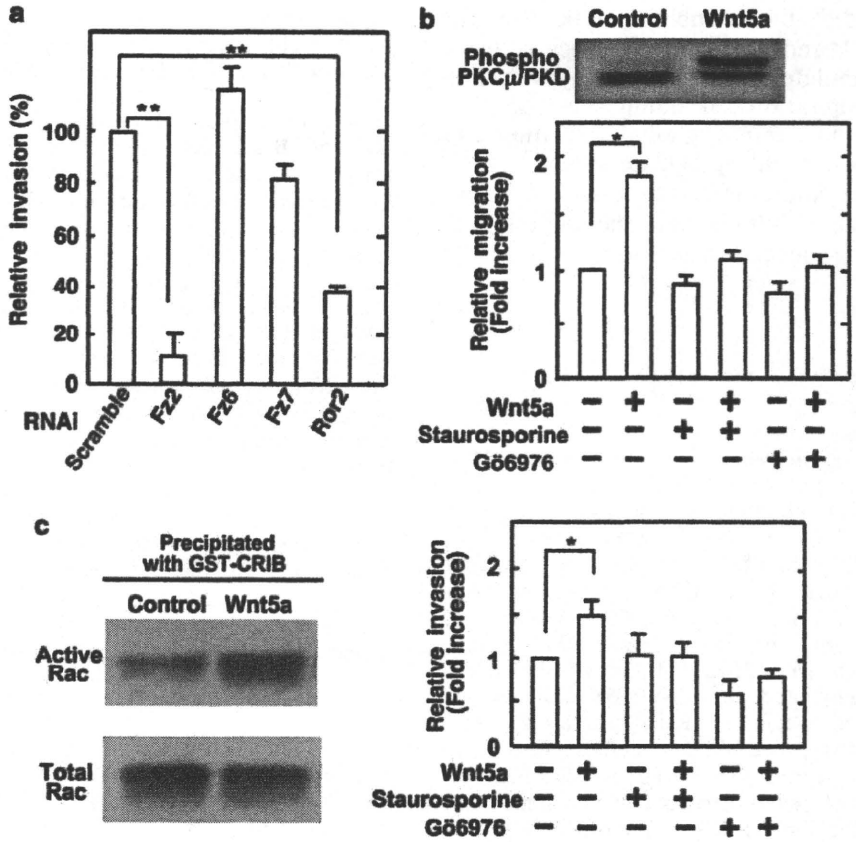

Figure 4 Wnt5a stimulates cell migration and invasion by activating protein kinase C (PKC). (**a**) DU145 cells transfected with *scrambled*, *Fz2*, *Fz6*, *Fz7* or *Ror2* siRNA were placed in Matrigel-coated transwell chambers for an invasion assay. In three independent fields, 37 ± 7 transfectants with *scrambled* siRNA invaded. Relative invasion activities were expressed as fold increases compared with the transfectants with *scrambled* siRNA. The results shown are means ± s.e. from three independent experiments. $^{**}P<0.01$. (**b**) Top panel, DU145 cells were stimulated with 300 ng/ml Wnt5a for 30 min, then the cell lysates were probed with anti-phospho protein kinase D (PKD)/PKCμ antibody. Middle panel, after DU145 cells were treated with 1.25 nM staurosporine or 100 nM Gö6976 for 2 h, the cells were subjected to the transwell migration assay in the presence or absence of 200 ng/ml Wnt5a. Relative migration activities were expressed as fold increases compared with that of cells in the absence of Wnt5a and without staurosporine. Bottom panel, after DU145 cells were treated with 2.5 nM staurosporine or 100 nM Gö6976 for 2 h, the cells were subjected to the Matrigel invasion assay in the presence or absence of 600 ng/ml Wnt5a. $^{*}P<0.05$. (**c**) DU145 cells were treated with 50 ng/ml Wnt5a for 1 h, and then cells were lyzed and probed with anti-Rac1 antibody. The same lysates were incubated with glutathione *S*-transferase (GST)-Cdc42/Rac-interacting binding domain (CRIB) immobilized on glutathione-sepharose to examine the activation of Rac. The total lysates and precipitates were probed with anti-Rac1 antibody. The results shown are representative of three independent experiments.

that the AP-1 site in the promoter region of the *MMP-1* gene is critical for its transcriptional regulation (Angel *et al.*, 1987) and that c-Jun and JunD bind to the AP-1 site (Doyle *et al.*, 1997; Wu *et al.*, 2006). In addition, knockdown of Fz2 and Ror2 reduced Wnt5a-dependent invasion and increment in *MMP-1* mRNA. From these results, it is suggested that the binding of Wnt5a to Fz2 and/or Ror2 stimulates the expression of MMP-1 by the recruitment of JunD to the AP-1 binding site of the promoter region of the *MMP-1* gene through the activation of PKC and JNK.

As shown in other cells (Kurayoshi *et al.*, 2006, 2007), Wnt5a activated Rac, which stimulates cell migration, in DU145 cells. However, the Wnt5a-Rac pathway was not involved in the expression of MMP-1. Therefore, it is also possible that Wnt5a activates Rac to stimulate cell migration independently of transcription and that this pathway cooperates with the Wnt5a/PKC pathway to stimulate cell invasion.

Although evidence has been accumulated that Wnt5a is expressed in various cancers (Weeraratna *et al.*, 2002; Veeman *et al.*, 2003; Huang *et al.*, 2005; Kurayoshi *et al.*, 2006; Pukrop *et al.*, 2006; Kikuchi and Yamamoto, 2008; Yamamoto *et al.*, 2009), how Wnt5a is upregulated in cancer cells has not been determined. It has been shown that Wnt5a is upregulated at the transcriptional level in PCa by hypomethylation in the 5′-untranslated region and that three CpG sites were consistently methylated in normal tissues but not in primary PCa (Wang *et al.*, 2007). It was also reported that membrane type 1-MMP is upregulated in PCa species and that membrane type 1-MMP-induced phenotypic changes are dependent on the expression of Wnt5a (Cao *et al.*, 2008). It is intriguing to speculate

that Wnt5a induced by membrane type 1-MMP upregulates MMP-1 and these three molecules work cooperatively to stimulate cell migration and invasion in PCa cells. Various alterations, including gene amplification, genetic mutations, transcriptional activation and epigenetic alterations, could upregulate Wnt5a expression in PCa. Further studies will be necessary to understand the functions of Wnt5a and the pathological significance of the abnormal expression of Wnt5a in cancer cells.

Materials and methods

Materials and chemicals

The *MMP-1* promoter-*luciferase* constructs and pGEX-αPAK-CRIB were provided by Dr I Clark (University of East Anglia, Norwich, UK) (Hall *et al.*, 2003) and Dr K Kaibuchi (Nagoya University, Nagoya, Japan), respectively. DU145, LNCap and PC3 cells were obtained from American Type Culture Collection (Manassas, VA, USA) and were grown in RPMI-1640 medium supplemented with 10% fetal bovine serum. PC3 cells stably expressing mouse Wnt5a were generated by selection with 200 μg/ml G418. Wnt5a was purified to homogeneity, and an anti-Wnt5a antibody was generated as described previously (Kurayoshi *et al.*, 2006, 2007). sFRP2 CM was prepared from culture medium of HEK293T cells stably expressing sFRP2 as described previously (Kurayoshi *et al.*, 2006). Control CM and Wnt5a CM were prepared as described previously (Kurayoshi *et al.*, 2007).

Immunohistochemistry

Formalin-fixed and paraffin-embedded samples were sectioned, deparaffinized and stained with hematoxylin and eosin to ensure that the sectioned block contained tumor cells. Adjacent sections were then stained immunohistochemically. For immunostaining of Wnt5a, a Dako CSA Kit (Dako, Carpinteria, CA, USA) was used according to the manufacturer's recommendation. Sections were pretreated in a microwave oven in citrate buffer for 30 min to retrieve antigenicity. After peroxidase activity was blocked with 3% H_2O_2-methanol for 10 min, the sections were incubated with normal goat serum (Dako) for 20 min to block nonspecific antibody binding sites. The anti-Wnt5a antibody was incubated with tissue samples for 15 min at room temperature and detected by incubating for 15 min with biotinylated goat anti-rabbit immunoglobulins, and the signal was amplified and visualized using the substrate-chromogen solution. The sections were counterstained with 0.1% hematoxylin. The specificity of the anti-Wnt5a antibody has been characterized previously (Kurayoshi *et al.*, 2006, 2007).

For immunostaining of β-catenin, a Dako LSAB Kit (Dako) was used in accordance with the manufacturer's recommendations. After blocking nonspecific antibody binding sites, the samples were incubated with mouse monoclonal anti-β-catenin (1:20; BD Bioscience, San Jose, CA, USA), and followed by incubation with biotinylated anti-mouse IgG and peroxidase-labeled streptavidin for 10 min each. Staining was completed with a 10-min incubation with the substrate-chromogen solution. The sections were counterstained with 0.1% hematoxylin. The staining of Wnt5a and cytosomal or nuclear β-catenin was classified according to the percentage of stained cancer cells in the tumor region. When more than 50% of cancer cells were stained, the immunostaining was considered positive.

Tissue samples

Ninety-eight primary tumors were collected from patients diagnosed with PCa who underwent surgery during the period 2000 through 2002 at the Department of Urology, Hiroshima University Hospital (Hiroshima, Japan). Identifying information for all samples was removed before analysis for strict privacy protection. This procedure was in accordance with the Ethical Guidelines for Human Genome/Gene Research of the Japanese Government, and the study was approved by the Ethical Committee for Human Genome Research of Hiroshima University (Hiroshima, Japan).

All patients were treated by radical prostatectomy and bilateral lymphadenectomy for clinically localized PCa and were confirmed to be node negative by pathological examination. None of the patients were treated preoperatively with hormonal or radiation therapy, and none had secondary cancer. All 98 specimens were archival, formalin-fixed and paraffin-embedded tissues. Tumor staging was performed according to the TNM classification system (Sobin and Wittekind, 2002). After prostatectomy, the serum PSA level was measured by E-test Tosoh II Assay (Tosoh, Tokyo, Japan). Patients were followed up by PSA measurement monthly during the first 6 months after prostatectomy and then every 3 months thereafter. Biochemical relapse was defined as a PSA level of 0.2 ng/ml or greater.

Statistical methods

Correlations between clinicopathological parameters and Wnt5a or β-catenin positivity were analyzed by Fisher's exact test. Kaplan–Meier curves were constructed, and differences between relapse-free survival curves were tested for statistical significance by log-rank test (Mantel, 1966). Cox proportional hazards multivariate model was used to examine the association of clinical and pathological factors and the expression of Wnt5a or β-catenin with relapse-free survival. Statistical analyses for Figures 3–5 were carried out using Student's *t*-test. A *P*-value of less than 0.05 was considered statistically significant.

Cell migration and invasion assays

To measure the cell migration activity, we performed transwell assays using a modified Boyden chamber (tissue culture treated, 6.5-mm-diameter, 10-μm-thickness, 8-μm-pores; Transwell, Costar, Cambridge, MA, USA) as described previously (Kobayashi *et al.*, 2006). The lower surface of the filters was coated with 10 μg/ml fibronectin for LNCap cells and 10 μg/ml type I collagen for DU145 cells. DU145 and LNCap cells (2.5×10^4 cells in 100 μl) suspended in serum-free RPMI-1640 medium containing 0.1% bovine serum albumin were applied to the upper chamber. The same medium was added to the lower chamber. After the cells were incubated at 37 °C for 4–8 h, the number of cells that migrated to the lower side of the upper chamber was counted. Relative cell migration was expressed as a percentage of migrated cells with siRNA treatment compared to those without treatment. The invasive potentials of DU145 and PC3 cells were analyzed using a Matrigel-coated modified Boyden chamber (Becton, Dickinson and Company, Bedford, MA, USA). RPMI-1640 medium containing 10% fetal bovine serum was added to the lower chamber. The incubations of DU145 and PC3 cells were continued for 24 and 4 h, respectively.

To carry out the wound-healing assay, we plated the cells onto fibronectin-coated coverslips. The monolayer of DU145 cells was then scratched manually with a plastic pipette tip, and after being washed with PBS, the wounded monolayers of

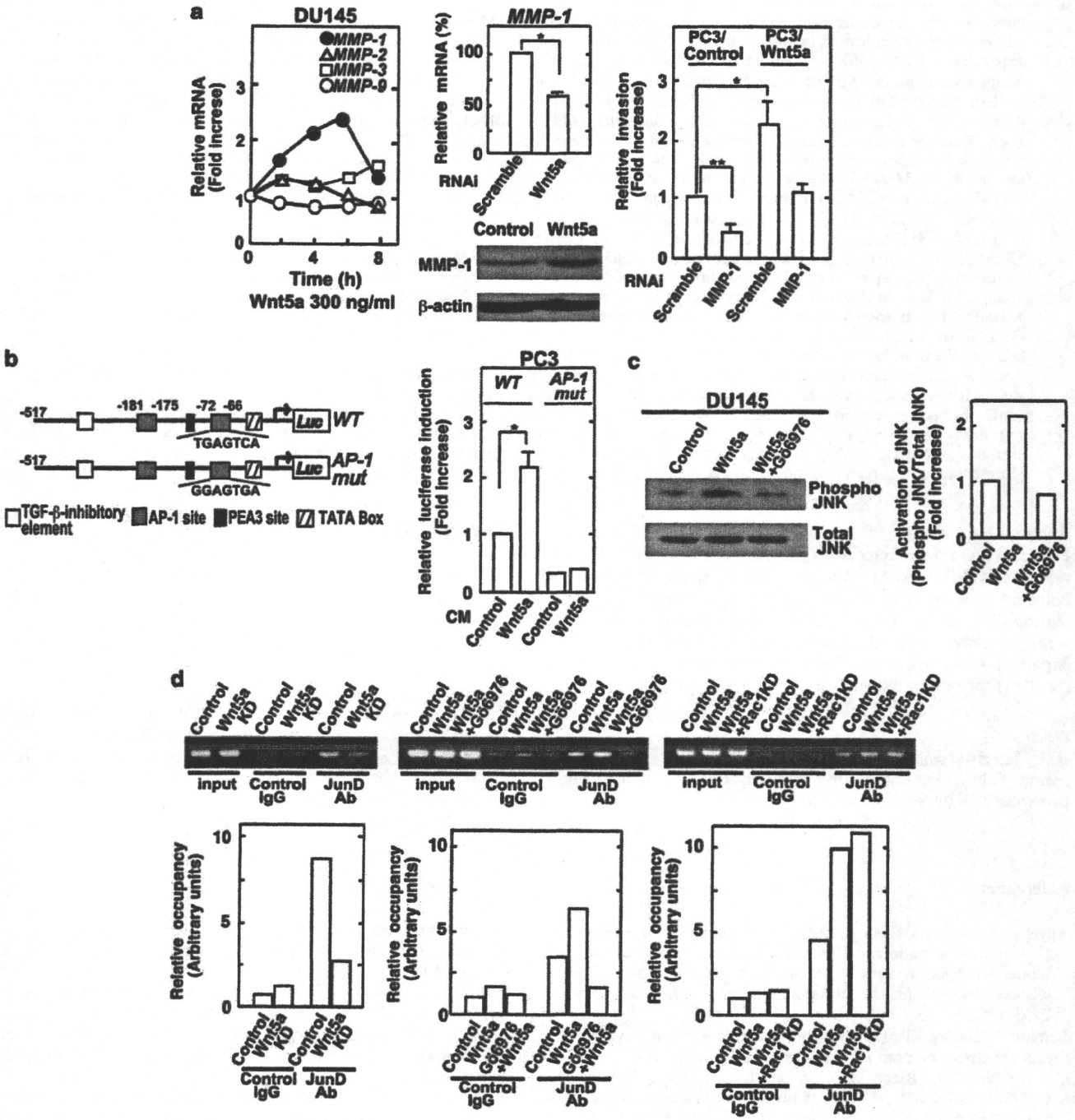

cells were allowed to heal for 18–24 h in RPMI-1640 medium containing 10% fetal bovine serum. The length of the wounds was measured and expressed as a percentage of the initial length at zero time (Kobayashi *et al*., 2006). When necessary, the anti-Wnt5a antibody (10 μg/ml) or CM containing sFRP2 was added to the medium.

Chromatin immunoprecipitation assay

Cells (2×10^6) were cross-linked with 1% formaldehyde for 10 min at room temperature. The cell pellets were lyzed with SDS lysis buffer and sonicated to shear DNA to a size range between 200 and 1000 bp. Sheared chromatin samples were diluted in chromatin immunoprecipitation buffer and incubated for 12 h at 4 °C with 6 μg of anti-JunD antibody (sc-74; Santa Cruz Biotechnology, Santa Cruz, CA, USA) or negative control IgG (Diagenode, Liège, Belgium). Immunocomplexes were collected, and the DNA fragments were purified using DNA purifying slurry (Diagenode). After incubation at 55 °C for 30 min to reverse protein/DNA cross-links, the purified DNA was used as a template for PCR. Forward and reverse primers were as follows: fragment containing AP-1 sites of *MMP-1* promoter, 5′-TGTCTCCTTCGCACACATCT-3′ and 5′-TGCATACTGGCCTTTGTCTT-3′.

Figure 5 Wnt5a induces the expression of matrix metalloproteinase-1 (MMP-1). (**a**) Left panel, DU145 cells were treated with 300 ng/ml Wnt5a for the indicated periods of time, and then *MMP-1*, *MMP-2*, *MMP-3* and *MMP-9* mRNA levels were quantified. Middle upper panel, *MMP-1* mRNA levels in DU145 cells transfected with *scrambled* or *Wnt5a* siRNA were quantified. The results shown are means ± s.e. from three independent experiments. $*P<0.05$. Middle lower panel, DU145 cells were stimulated with 300 ng/ml Wnt5a for 10 h, then the cell lysates were probed with anti-MMP-1 antibody. β-Actin is a loading control. Right panel, PC3/control and PC3/Wnt5a cells were transfected transiently with *scrambled* or *MMP-1* siRNA, and these cells were subjected to the Matrigel invasion assay. Relative invasion activities were expressed as fold increases compared with the invaded cell numbers in PC3/control cells transfected with *scrambled* siRNA. The results shown are means ± s.e. from three independent experiments. $*P<0.05$; $**P<0.01$. (**b**) Left panel, the *MMP-1-luciferase* constructs used in this study. Right panel, after PC3 cells were transfected with pGL3/*MMP-1 −517/+60-Luc* with or without mutations in the proximal activator protein-1 (AP-1) site (*AP-1 mut* or *WT*, respectively), the cells were stimulated with control or Wnt5a conditioned medium (CM) for 10 h. Luciferase activities were expressed as fold increases compared with that of *WT* transfectants treated with control CM. The results shown are means ± s.e. from three independent experiments. $*P<0.05$. WT, wild type. (**c**) After the treatment of Gö6976 for 2 h, DU145 cells were stimulated with 450 ng/ml Wnt5a for 1 h. The cell lysates were probed with anti-phospho-c-jun N-terminal kinase (JNK) antibody. Right panel, the activity of JNK was calculated by dividing the band intensity of phosphorylated JNK by that of total JNK and expressed as fold increases compared with control DU145 cells. The results shown are representative of three independent experiments. (**d**) Left panel, chromatins from DU145/control and DU145/Wnt5aKD cells were immunoprecipitated with anti-JunD antibody or control IgG. KD, knockdown. Middle panel, after DU145 cells were stimulated with 450 ng/ml Wnt5a for 1 h in the presence or absence of 100 nM Gö6976, chromatins were collected and were immunoprecipitated with anti-JunD antibody or control IgG. Right panel, after DU145 cells were transfected with *scrambled* or *Rac1* siRNA, the cells were stimulated with 450 ng/ml Wnt5a for 1 h. Chromatins from each cell were immunoprecipitated with anti-JunD antibody or control IgG. The immunoprecipitated samples were analyzed by real-time PCR for the *MMP-1* promoter region containing two AP-1 sites. The relative amounts of DNA fragments containing AP-1 sites immunoprecipitated with anti-JunD antibody were expressed as arbitrary units compared with that with control IgG in control DU145 cells. The results shown are representative of three independent experiments.

Reporter gene assay

PC3 cells were transfected with pGL3/*MMP-1 −517/+60-Luc* and pME18S/LacZ. At 24 h after transfection, the cells were cultured in serum-free medium for 24 h and stimulated with Wnt5a CM for further 10 h, and then the luciferase activities were measured with PicaGene reagent (Toyo Ink, Tokyo, Japan). β-Galactosidase activities were determined to normalize the transfection efficiency.

Others

Rac activity was assayed using glutathione *S*-transferase fusion Cdc42/Rac-interacting binding domain as described previously (Kurayoshi *et al*., 2006).

Conflict of interest

The authors declare no conflict of interest.

Acknowledgements

This work was supported by Grants-in-Aid for Scientific Research and for Scientific Research on Priority Areas from the Ministry of Education, Science, and Culture of Japan (2007, 2008, 2009), The YASUDA Medical Foundation (2006) and Uehara Memorial Foundation (2008).

References

Angel P, Baumann I, Stein B, Delius H, Rahmsdorf HJ, Herrlich P. (1987). 12-*O*-tetradecanoyl-phorbol-13-acetate induction of the human collagenase gene is mediated by an inducible enhancer element located in the 5′-flanking region. *Mol Cell Biol* **7**: 2256–2266.

Bernard P, Harley VR. (2007). Wnt4 action in gonadal development and sex determination. *Int J Biochem Cell Biol* **39**: 31–43.

Cao J, Chiarelli C, Richman O, Zarrabi K, Kozarekar P, Zucker S. (2008). Membrane type 1 matrix metalloproteinase induces epithelial-to-mesenchymal transition in prostate cancer. *J Biol Chem* **283**: 6232–6240.

D'Amico AV, Whittington R, Malkowicz SB, Schultz D, Fondurulia J, Chen MH *et al.* (2000). Clinical utility of the percentage of positive prostate biopsies in defining biochemical outcome after radical prostatectomy for patients with clinically localized prostate cancer. *J Clin Oncol* **18**: 1164–1172.

Dejmek J, Dejmek A, Safholm A, Sjolander A, Andersson T. (2005). Wnt-5a protein expression in primary dukes B colon cancers identifies a subgroup of patients with good prognosis. *Cancer Res* **65**: 9142–9146.

Doyle GA, Pierce RA, Parks WC. (1997). Transcriptional induction of collagenase-1 in differentiated monocyte-like (U937) cells is regulated by AP-1 and an upstream C/EBP-β site. *J Biol Chem* **272**: 11840–11849.

Egeblad M, Werb Z. (2002). New functions for the matrix metalloproteinases in cancer progression. *Nat Rev Cancer* **2**: 161–174.

Gleason DF, Mellinger GT. (1974). Prediction of prognosis for prostatic adenocarcinoma by combined histological grading and clinical staging. *J Urol* **111**: 58–64.

Hall MC, Young DA, Waters JG, Rowan AD, Chantry A, Edwards DR *et al.* (2003). The comparative role of activator protein 1 and Smad factors in the regulation of Timp-1 and MMP-1 gene expression by transforming growth factor-β1. *J Biol Chem* **278**: 10304–10313.

Han M, Partin AW, Zahurak M, Piantadosi S, Epstein JI, Walsh PC. (2003). Biochemical (prostate specific antigen) recurrence probability following radical prostatectomy for clinically localized prostate cancer. *J Urol* **169**: 517–523.

Hart CA, Scott LJ, Bagley S, Bryden AA, Clarke NW, Lang SH. (2002). Role of proteolytic enzymes in human prostate bone metastasis formation: *in vivo* and *in vitro* studies. *Br J Cancer* **86**: 1136–1142.

Hsing AW, Tsao L, Devesa SS. (2000). International trends and patterns of prostate cancer incidence and mortality. *Int J Cancer* **85**: 60–67.

Huang CL, Liu D, Nakano J, Ishikawa S, Kontani K, Yokomise H *et al.* (2005). Wnt5a expression is associated with the tumor proliferation and the stromal vascular endothelial growth factor—an expression in non-small-cell lung cancer. *J Clin Oncol* **23**: 8765–8773.

Hurlstone A, Clevers H. (2002). T-cell factors: turn-ons and turn-offs. *EMBO J* **21**: 2303–2311.

Jemal A, Siegel R, Ward E, Hao Y, Xu J, Murray T *et al.* (2008). Cancer statistics, 2008. *CA Cancer J Clin* **58**: 71–96.

Kawano Y, Kypta R. (2003). Secreted antagonists of the Wnt signalling pathway. *J Cell Sci* **116**: 2627–2634.

Kikuchi A. (2003). Tumor formation by genetic mutations in the components of the Wnt signaling pathway. *Cancer Sci* **94**: 225–229.

Kikuchi A, Yamamoto H. (2008). Tumor formation due to abnormalities in the β-catenin-independent pathway of Wnt signaling. *Cancer Sci* **99**: 202–208.

Kikuchi A, Yamamoto H, Sato A. (2009). Selective activation mechanisms of Wnt signaling pathways. *Trends Cell Biol* **19**: 119–129.

Kobayashi T, Hino S-I, Oue N, Asahara T, Zollo M, Yasui W *et al.* (2006). Glycogen synthase kinase 3 and h-prune regulate cell migration by modulating focal adhesions. *Mol Cell Biol* **26**: 898–911.

Kremenevskaja N, von Wasielewski R, Rao AS, Schofl C, Andersson T, Brabant G. (2005). Wnt-5a has tumor suppressor activity in thyroid carcinoma. *Oncogene* **24**: 2144–2154.

Kurayoshi M, Oue N, Yamamoto H, Kishida M, Inoue A, Asahara T *et al.* (2006). Expression of Wnt-5a is correlated with aggressiveness of gastric cancer by stimulating cell migration and invasion. *Cancer Res* **66**: 10439–10448.

Kurayoshi M, Yamamoto H, Izumi S, Kikuchi A. (2007). Post-translational palmitoylation and glycosylation of Wnt-5a are necessary for its signalling. *Biochem J* **402**: 515–523.

Logan CY, Nusse R. (2004). The Wnt signaling pathway in development and disease. *Annu Rev Cell Dev Biol* **20**: 781–810.

Mantel N. (1966). Evaluation of survival data and two new rank order statistics arising in its consideration. *Cancer Chemother Rep* **50**: 163–170.

Masckauchan TN, Agalliu D, Vorontchikhina M, Ahn A, Parmalee NL, Li CM *et al.* (2006). Wnt5a signaling induces proliferation and survival of endothelial cells *in vitro* and expression of MMP-1 and Tie-2. *Mol Biol Cell* **17**: 5163–5172.

Oishi I, Suzuki H, Onishi N, Takada R, Kani S, Ohkawara B *et al.* (2003). The receptor tyrosine kinase Ror2 is involved in non-canonical Wnt5a/JNK signalling pathway. *Genes Cells* **8**: 645–654.

Partin AW, Kattan MW, Subong EN, Walsh PC, Wojno KJ, Oesterling JE *et al.* (1997). Combination of prostate-specific antigen, clinical stage, and Gleason score to predict pathological stage of localized prostate cancer. A multi-institutional update. *JAMA* **277**: 1445–1451.

Polakis P. (2000). Wnt signaling and cancer. *Genes Dev* **14**: 1837–1851.

Pound CR, Partin AW, Eisenberger MA, Chan DW, Pearson JD, Walsh PC. (1999). Natural history of progression after PSA elevation following radical prostatectomy. *JAMA* **281**: 1591–1597.

Pukrop T, Klemm F, Hagemann T, Gradl D, Schulz M, Siemes S *et al.* (2006). Wnt 5a signaling is critical for macrophage-induced invasion of breast cancer cell lines. *Proc Natl Acad Sci USA* **103**: 5454–5459.

Rozengurt E, Rey O, Waldron RT. (2005). Protein kinase D signaling. *J Biol Chem* **280**: 13205–13208.

Sato A, Yamamoto H, Sakane H, Koyama H, Kikuchi A. (2010). Wnt5a regulates distinct signaling pathways by binding to Frizzled2. *EMBO J* **29**: 41–54.

Sobin LH, Wittekind CH. (2002). *TNM Classification of Malignant Tumors*, 6th edn. Wiley-Liss, Inc.: New York.

Stanbrough M, Bubley GJ, Ross K, Golub TR, Rubin MA, Penning TM *et al.* (2006). Increased expression of genes converting adrenal androgens to testosterone in androgen-independent prostate cancer. *Cancer Res* **66**: 2815–2825.

Veeman MT, Axelrod JD, Moon RT. (2003). A second canon. Functions and mechanisms of β-catenin-independent Wnt signaling. *Dev Cell* **5**: 367–377.

Verras M, Brown J, Li X, Nusse R, Sun Z. (2004). Wnt3a growth factor induces androgen receptor-mediated transcription and enhances cell growth in human prostate cancer cells. *Cancer Res* **64**: 8860–8866.

Wang HY, Liu T, Malbon CC. (2006). Structure-function analysis of Frizzleds. *Cell Signal* **18**: 934–941.

Wang Q, Williamson M, Bott S, Brookman-Amissah N, Freeman A, Nariculam J *et al.* (2007). Hypomethylation of WNT5A, CRIP1 and S100P in prostate cancer. *Oncogene* **26**: 6560–6565.

Weeraratna AT, Jiang Y, Hostetter G, Rosenblatt K, Duray P, Bittner M *et al.* (2002). Wnt5a signaling directly affects cell motility and invasion of metastatic melanoma. *Cancer Cell* **1**: 279–288.

Wu JY, Lu H, Sun Y, Graham DY, Cheung HS, Yamaoka Y. (2006). Balance between polyoma enhancing activator 3 and activator protein 1 regulates *Helicobacter pylori*-stimulated matrix metalloproteinase 1 expression. *Cancer Res* **66**: 5111–5120.

Yamamoto H, Kitadai Y, Oue N, Ohdan H, Yasui W, Kikuchi A. (2009). Laminin γ2 mediates Wnt5a-induced invasion of gastric cancer cells. *Gastroenterology* **137**: 242–252, 252 e241-246.

Yardy GW, Brewster SF. (2005). Wnt signalling and prostate cancer. *Prostate Cancer Prostatic Dis* **8**: 119–126.

Zeng ZZ, Jia Y, Hahn NJ, Markwart SM, Rockwood KF, Livant DL. (2006). Role of focal adhesion kinase and phosphatidylinositol 3′-kinase in integrin fibronectin receptor-mediated, matrix metalloproteinase-1-dependent invasion by metastatic prostate cancer cells. *Cancer Res* **66**: 8091–8099.

Supplementary Information accompanies the paper on the Oncogene website (http://www.nature.com/onc)